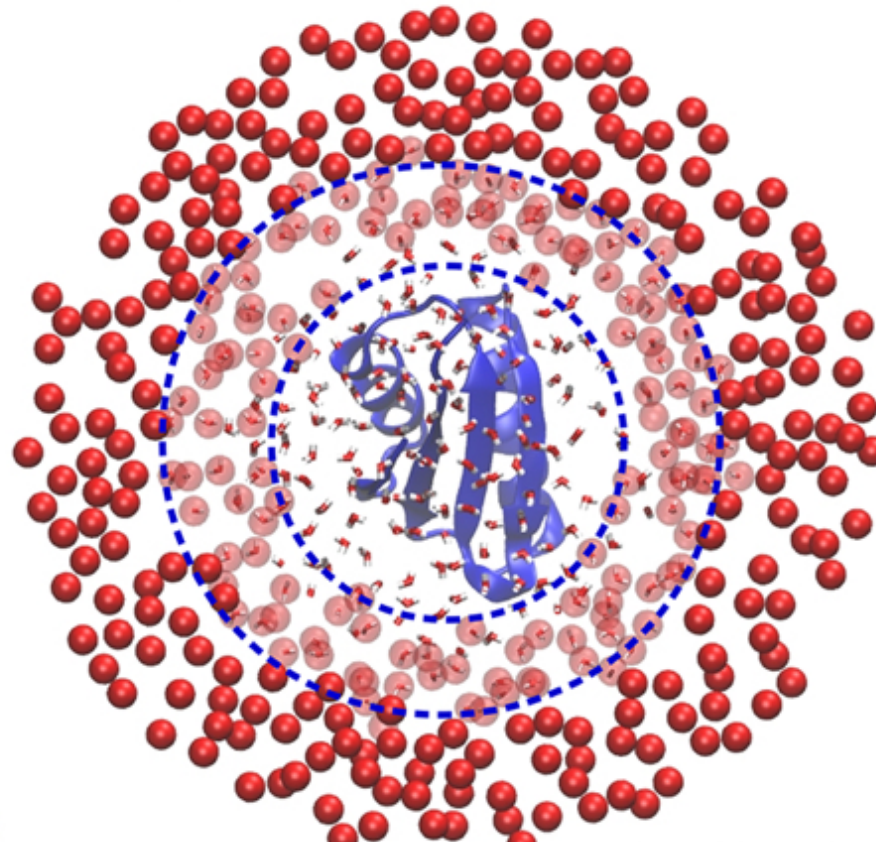


The devil is in the atomistic detail

Problems and solutions in computational soft matter



Raffaello Potestio

University of Trento | Physics Department
TIFPA - Trento Institute for Fundamental Physics and Applications

Acknowledgements

MPIP Mainz

PhD Students

Sebastian Fritsch
Karsten Kreis
Maziar Heidari
Raffaele Fiorentini

PostDocs

Aoife C. Fogarty
Robinson Cortes-Huerto

PI's

Kurt Kremer
Davide Donadio

Collaborators

Rosa Bulo (Utrecht)
Rafael Delgado Buscalioni (Madrid)
Pep Español (Madrid)
Ralf Everaers (Lyon)
Mark E. Tuckerman (New York)
Paolo Carloni (Jülich)

Funding and support





Table of contents



Table of contents

- Intro: the multi-scale challenge



Table of contents

- Intro: the multi-scale challenge
- Modelling and coarse-graining methods



Table of contents

- Intro: the multi-scale challenge
- Modelling and coarse-graining methods
- Dual-resolution models of liquids (AdResS, H-AdResS)



Table of contents

- Intro: the multi-scale challenge
- Modelling and coarse-graining methods
- Dual-resolution models of liquids (AdResS, H-AdResS)
- Application of (H-)AdResS in chemical and biological physics



Table of contents

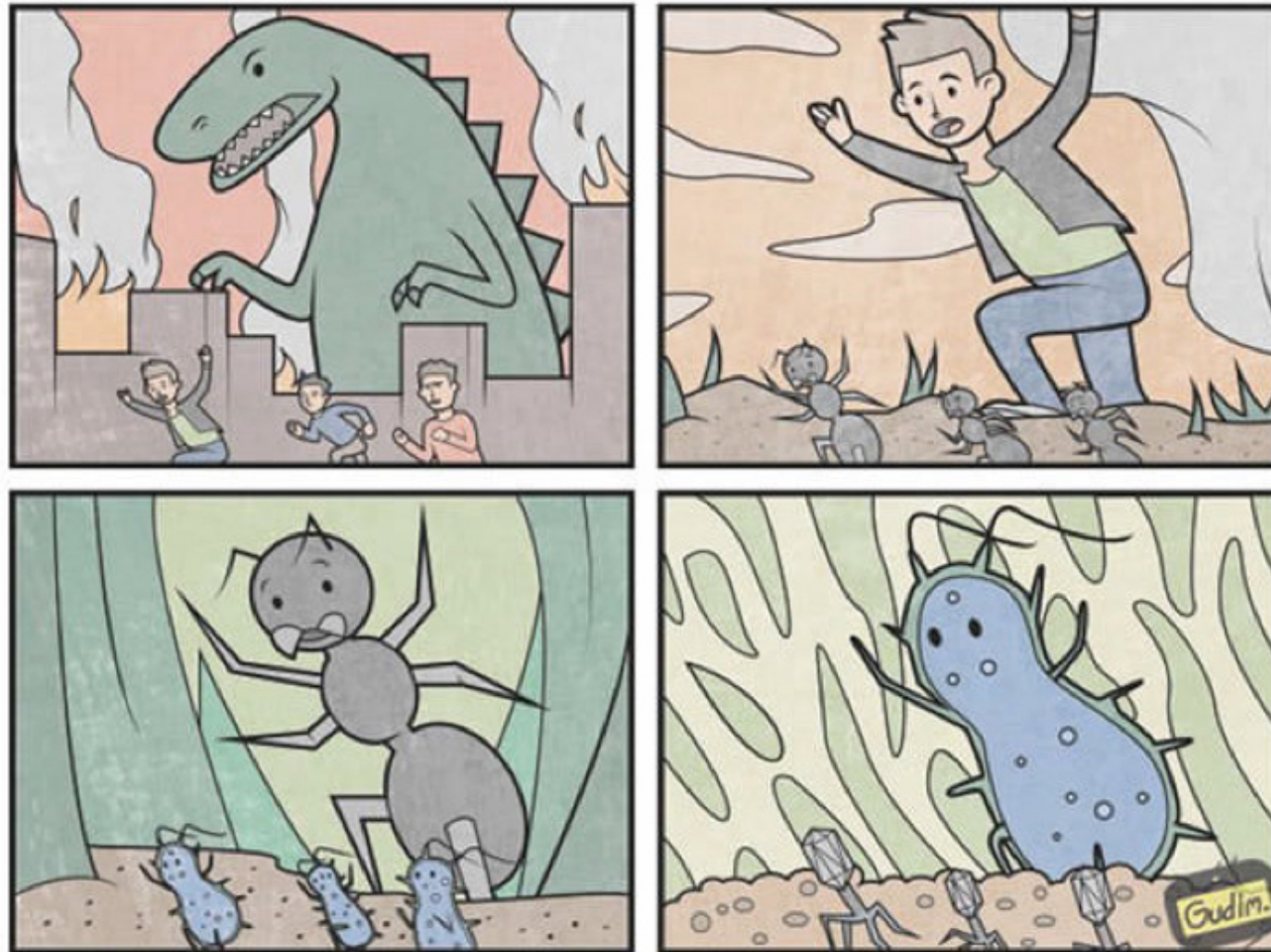
- Intro: the multi-scale challenge
- Modelling and coarse-graining methods
- Dual-resolution models of liquids (AdResS, H-AdResS)
- Application of (H-)AdResS in chemical and biological physics
- Dual-resolution models of proteins



Table of contents

- Intro: the multi-scale challenge
- Modelling and coarse-graining methods
- Dual-resolution models of liquids (AdResS, H-AdResS)
- Application of (H-)AdResS in chemical and biological physics
- Dual-resolution models of proteins
- Conclusions and perspectives

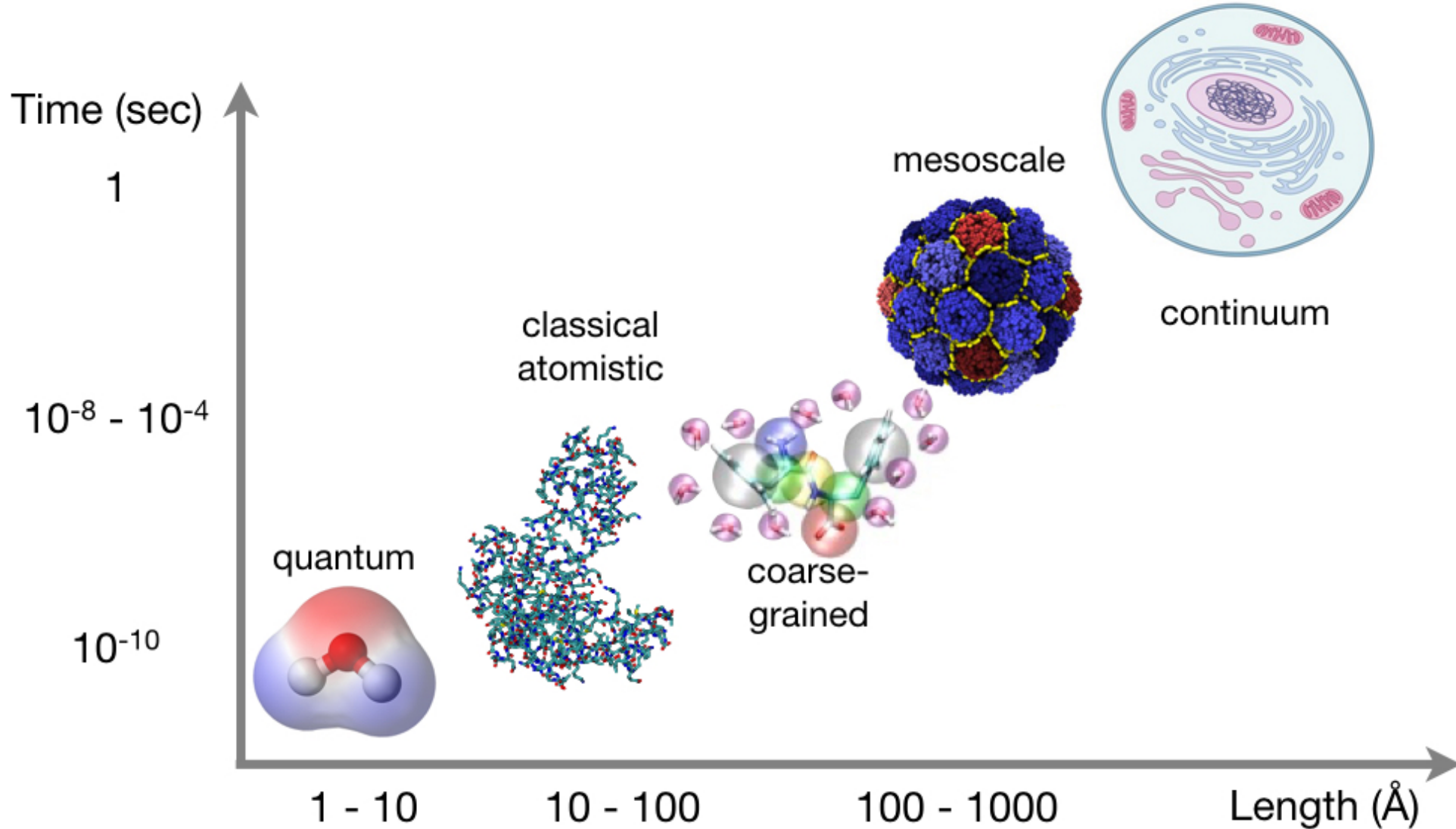
Motivation: the multiscale challenge in biological systems



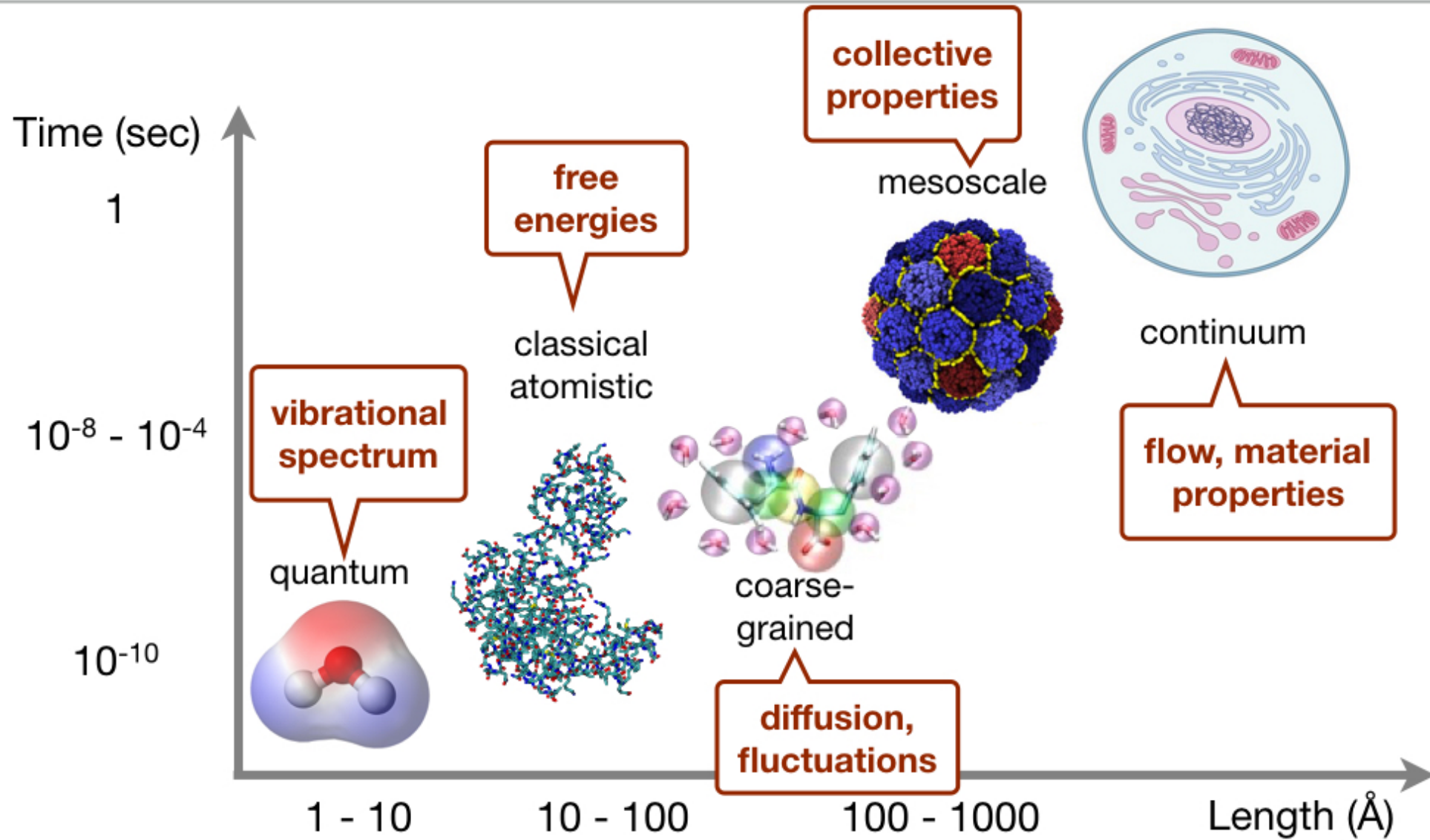
Motivation: the multiscale challenge in biological systems



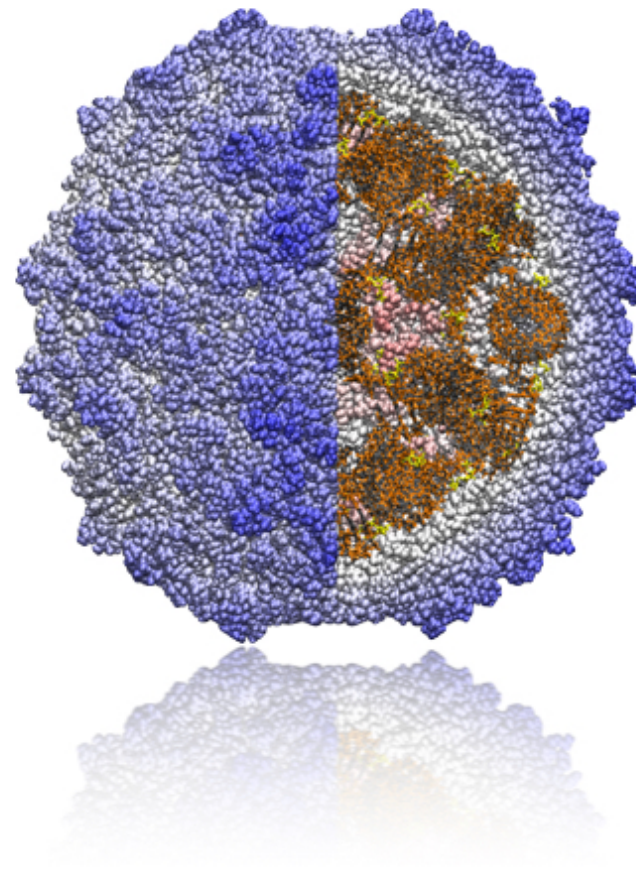
Motivation: the multiscale challenge in biological systems



Motivation: the multiscale challenge in biological systems



Motivation: the multiscale challenge in biological systems



Fully atomistic simulation
of viral capsids (e.g. [1])

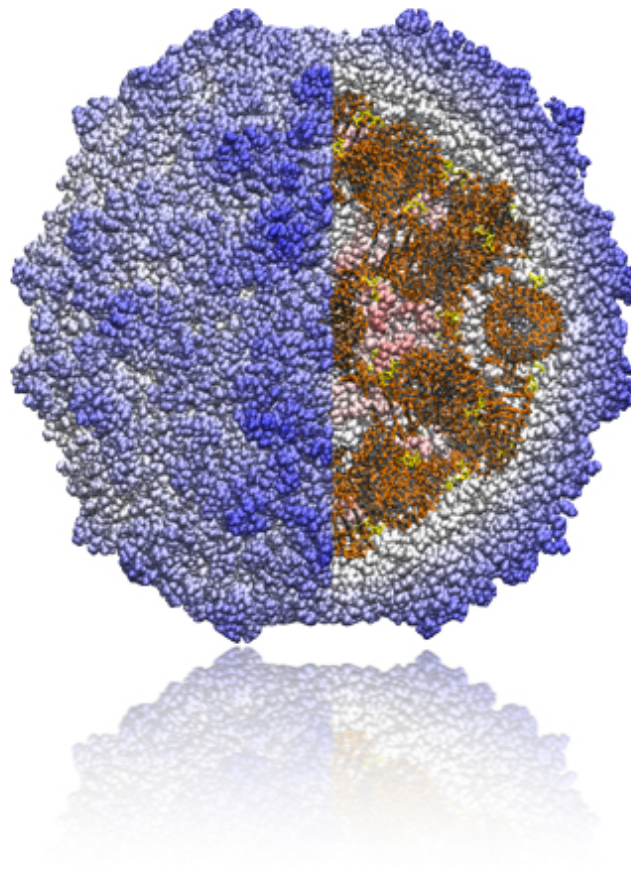
- 10^6 atoms
-simulation duration: ~100ns

[1] P.L. Freddolino, A.S. Arkhipov, S.B. Larson, A. McPherson, K. Schulten, Structure 14, 2006

Motivation: the multiscale challenge in biological systems

Fully atomistic simulation
of viral capsids (e.g. [1])

- 10^6 atoms
-simulation duration: ~100ns



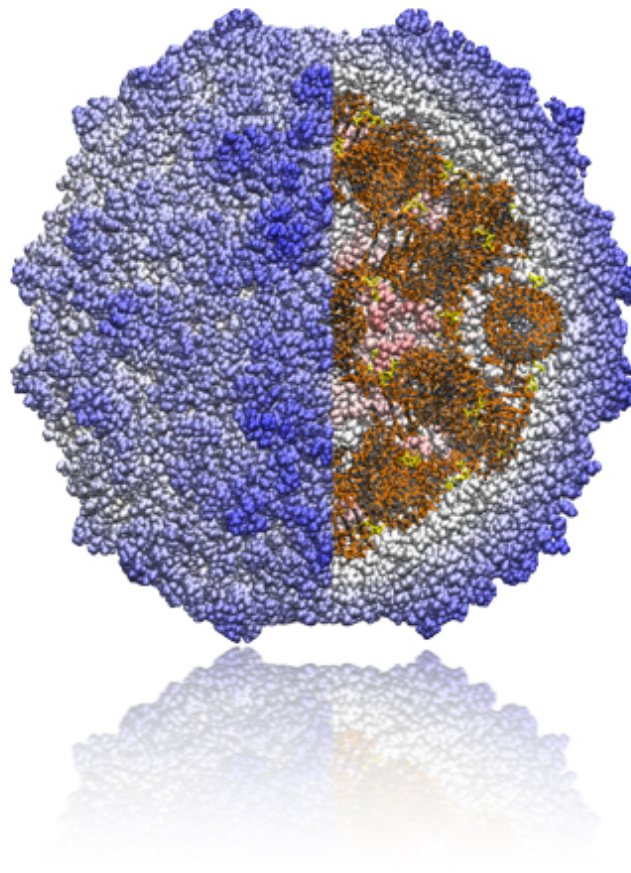
- Practical limitations
(e.g. \$\$\$, time)

[1] P.L. Freddolino, A.S. Arkhipov, S.B. Larson, A. McPherson, K. Schulten, Structure 14, 2006

Motivation: the multiscale challenge in biological systems

Fully atomistic simulation
of viral capsids (e.g. [1])

- 10^6 atoms
-simulation duration: ~100ns



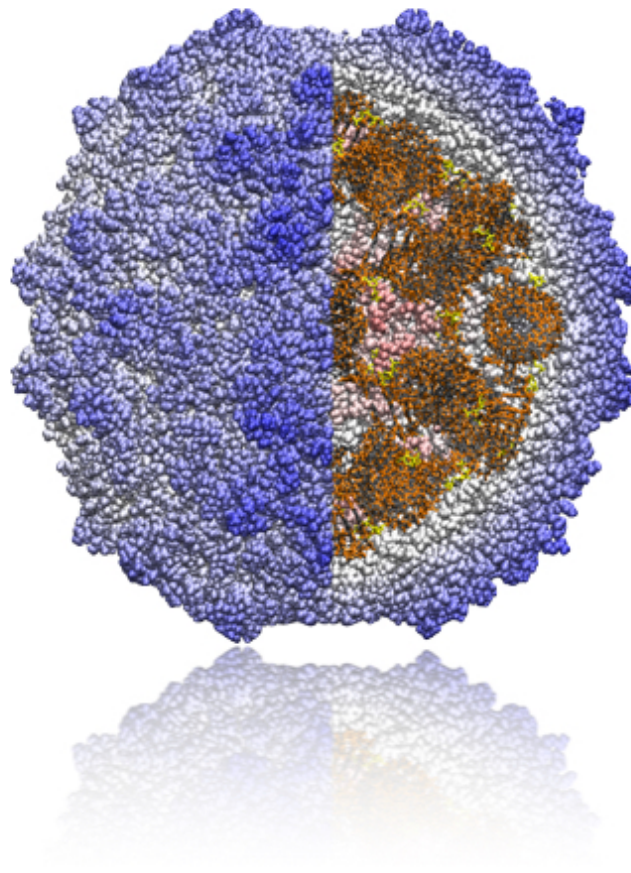
- Practical limitations
(e.g. \$\$\$, time)
- Get more insight at
modeling stage

[1] P.L. Freddolino, A.S. Arkhipov, S.B. Larson, A. McPherson, K. Schulten, Structure 14, 2006

Motivation: the multiscale challenge in biological systems

Fully atomistic simulation
of viral capsids (e.g. [1])

- 10^6 atoms
-simulation duration: ~100ns

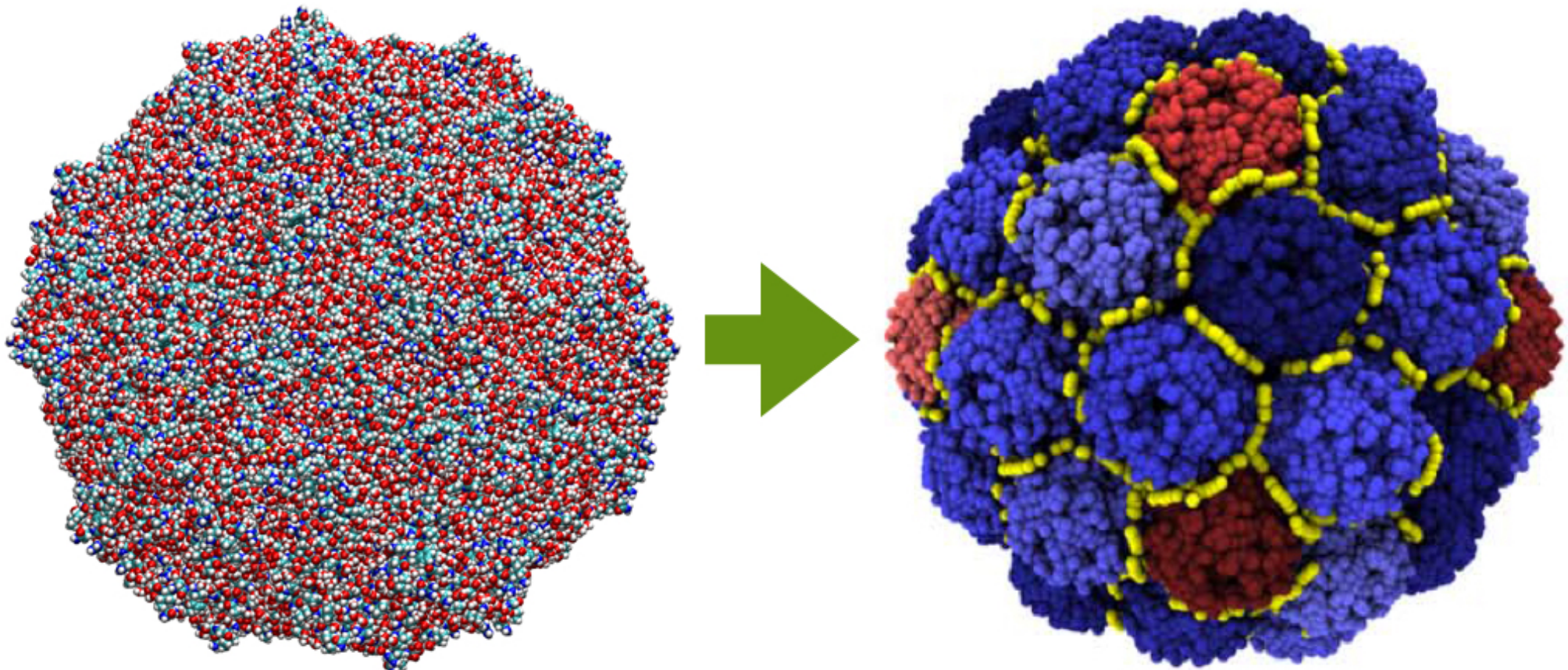


- Practical limitations (e.g. \$\$\$, time)
- Get more insight at modeling stage
- Explore the parameter space

[1] P.L. Freddolino, A.S. Arkhipov, S.B. Larson, A. McPherson, K. Schulten, Structure 14, 2006

Modelling as a source of insight

“It is nice to know that the computer understands the problem.
But I would like to understand it, too.”
[Eugene Wigner]

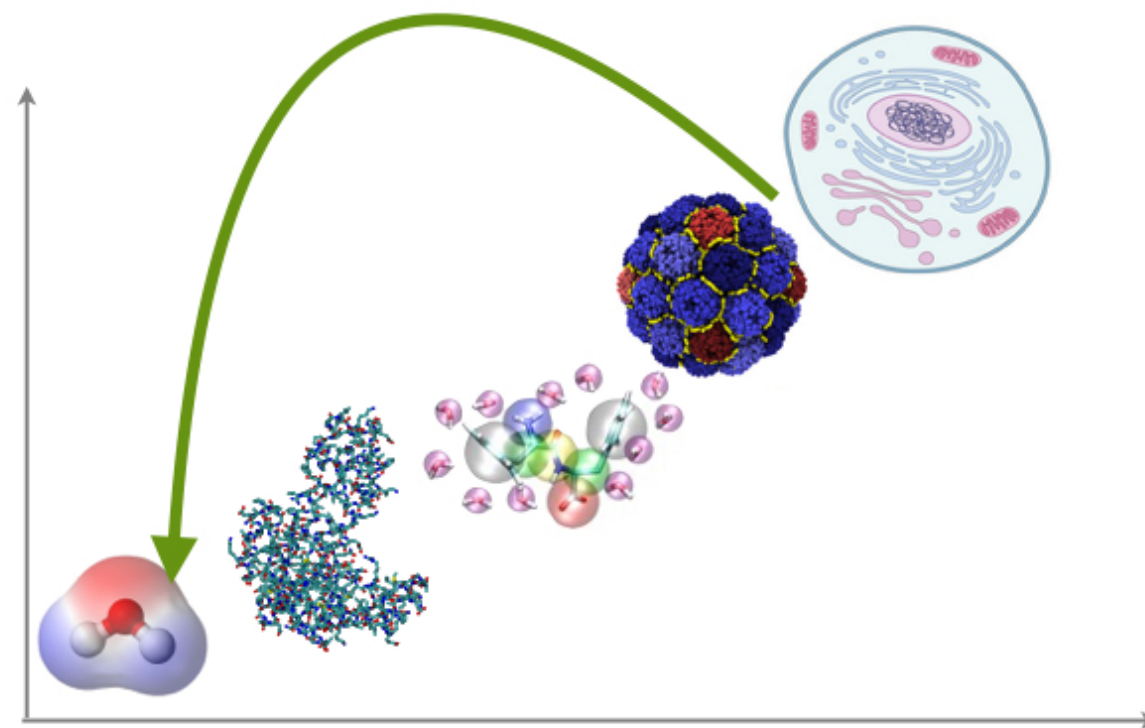


Coarse-graining methods in soft matter



TOP-DOWN APPROACHES

Higher-level knowledge is employed
to parametrize system interactions



Coarse-graining methods in soft matter



TOP-DOWN APPROACHES

Higher-level knowledge is employed
to parametrize system interactions

Elastic Network Models

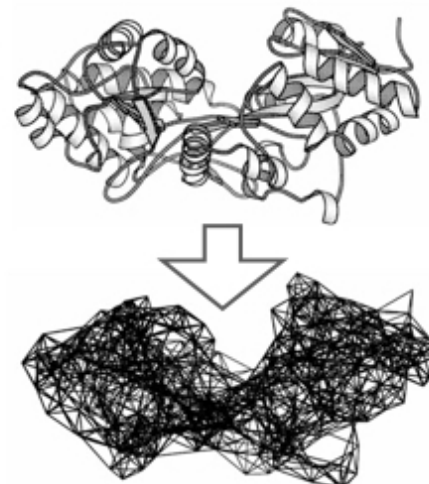
The collective dynamics emerges from
a large number of small-scale interactions

$$E_p = \frac{1}{2} \sum_{\text{bonds}} K_b(b - b_0)^2 + \frac{1}{2} \sum_{\text{angles}} K_\theta(\theta - \theta_0)^2 + \frac{1}{2} \sum_{\text{dihedrals}} K_\phi[1 + \cos(n\phi - \delta)] + \sum_{\text{non bonded pairs}} \left[\frac{A}{r^{12}} - \frac{B}{r^6} + \frac{q_1 q_2}{Dr} \right]. \quad (1)$$

$$E(\mathbf{r}_a, \mathbf{r}_b) = \frac{C}{2} \left(\frac{\mathbf{r}_{a,b}^0 \cdot \Delta \mathbf{r}_{a,b}}{|\mathbf{r}_{a,b}^0|} \right)^2$$

M. Tirion, PRL (1996)

Figure by YH Sanejouand, from Monticelli and Saonen, Springer



Go Models

“Teleological” approach: interaction strength
determined by the folded 3D structure

Taketomi, Ueda, Go, Int J Pept Protein Res, 7, 445 (1975)

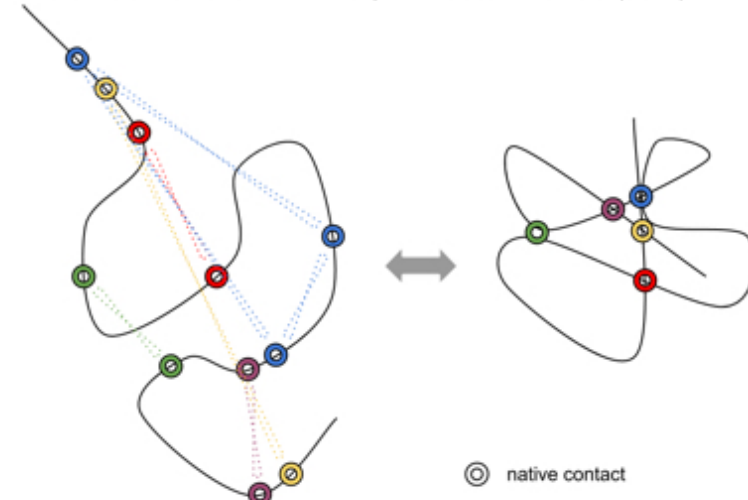


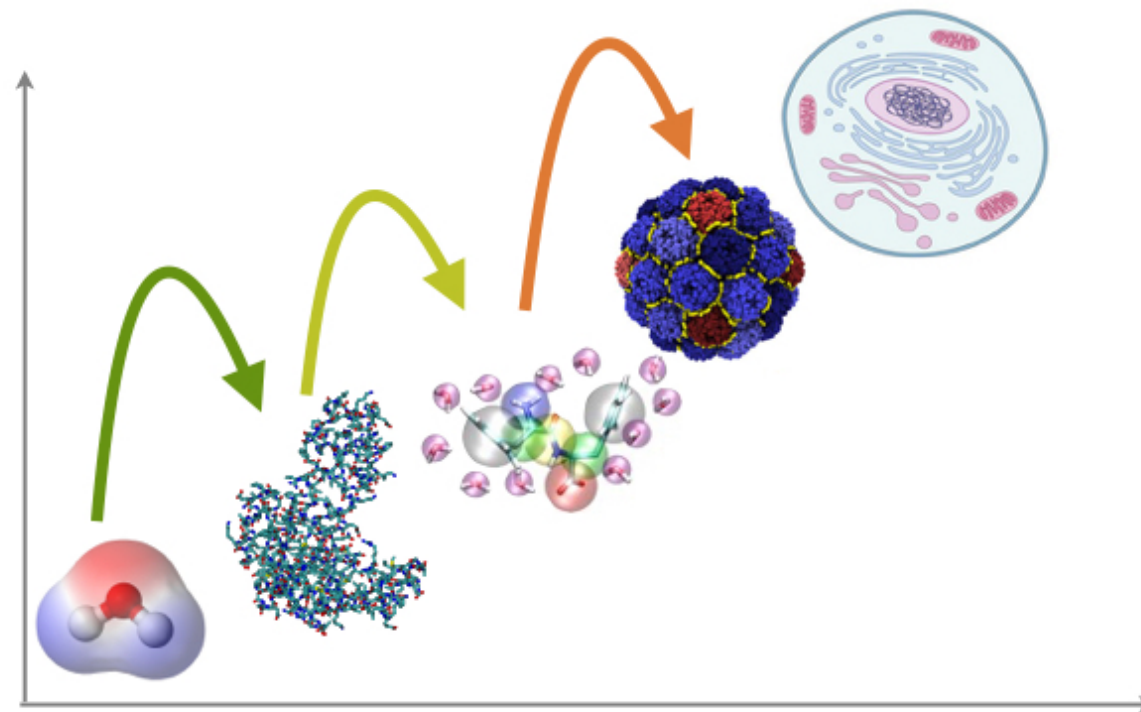
Figure by S. Demharter <http://www.blopig.com/blog/2014/03/journal-club-the-role-of-native-contacts-in-folding-of-small-proteins/>

Coarse-graining methods in soft matter



BOTTOM-UP APPROACHES OR SYSTEMATIC COARSE-GRAINING

Systematic inclusion of higher-resolution details into effective interactions among coarse-grained sites

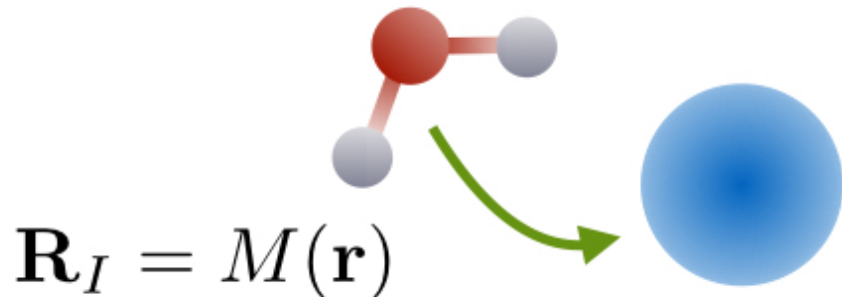


Coarse-graining methods in soft matter



Systematic CG'ing requires:

- **a mapping function**



- **a consistency criterion**

$$p_R(\mathbf{R}) = \langle \delta(M(\mathbf{r}) - \mathbf{R}) \rangle$$

$$P_R(\mathbf{R}) = p_R(\mathbf{R})$$

Multi-body PMF $U(\mathbf{R}) = -k_B T \ln z(\mathbf{R})$

$$z(\mathbf{R}) = \int d\mathbf{r} \exp[-u(\mathbf{r})/k_B T] \delta(M(\mathbf{r}) - \mathbf{R})$$

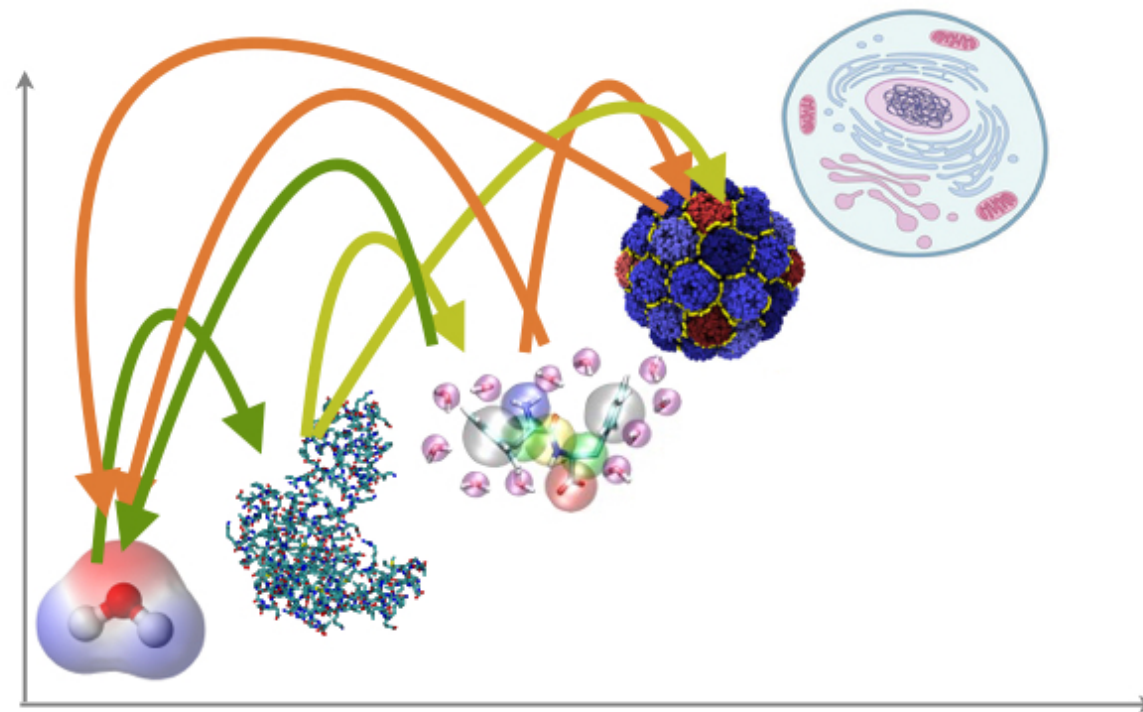
The big issue: approximate the MB PMF

Coarse-graining methods in soft matter



CONCURRENT MULTI-RESOLUTION APPROACHES

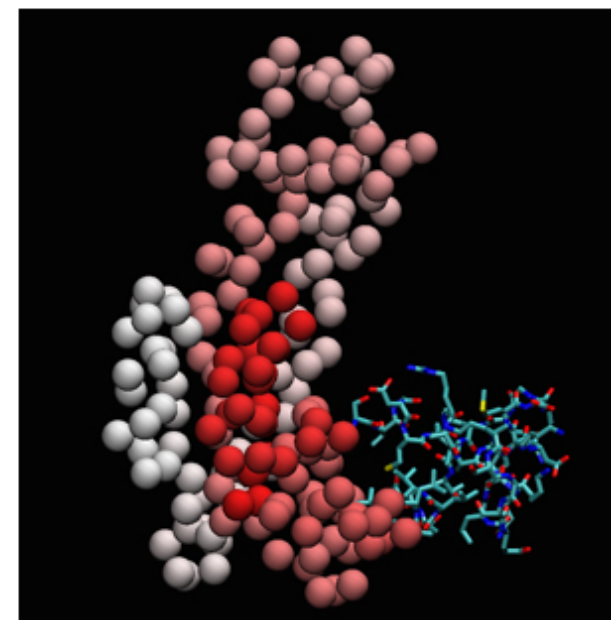
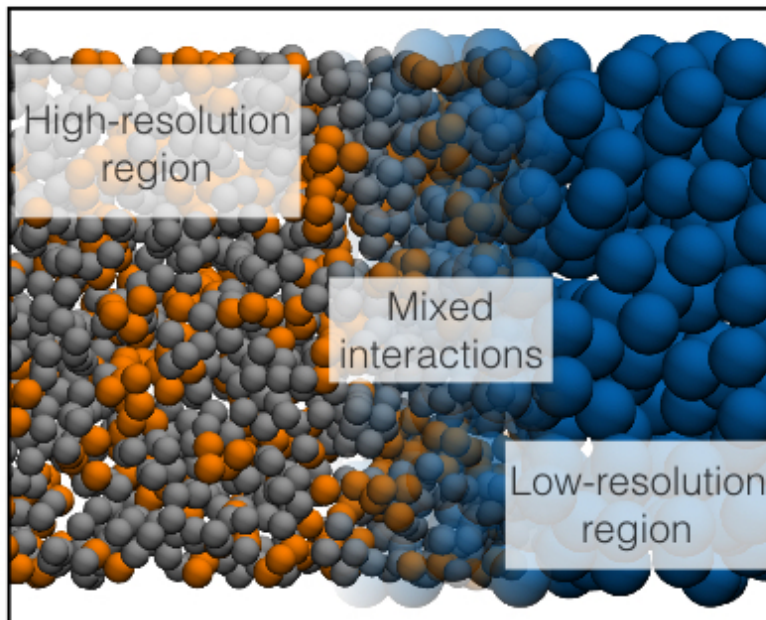
Interplay and feedback between different scales
No effective decoupling possible



Concurrent multi-resolution approaches

In principle the **highest resolution level** has to be retained

Alternative solution available if there is a **spatial separation** between the **interesting** and the **necessary** DoFs



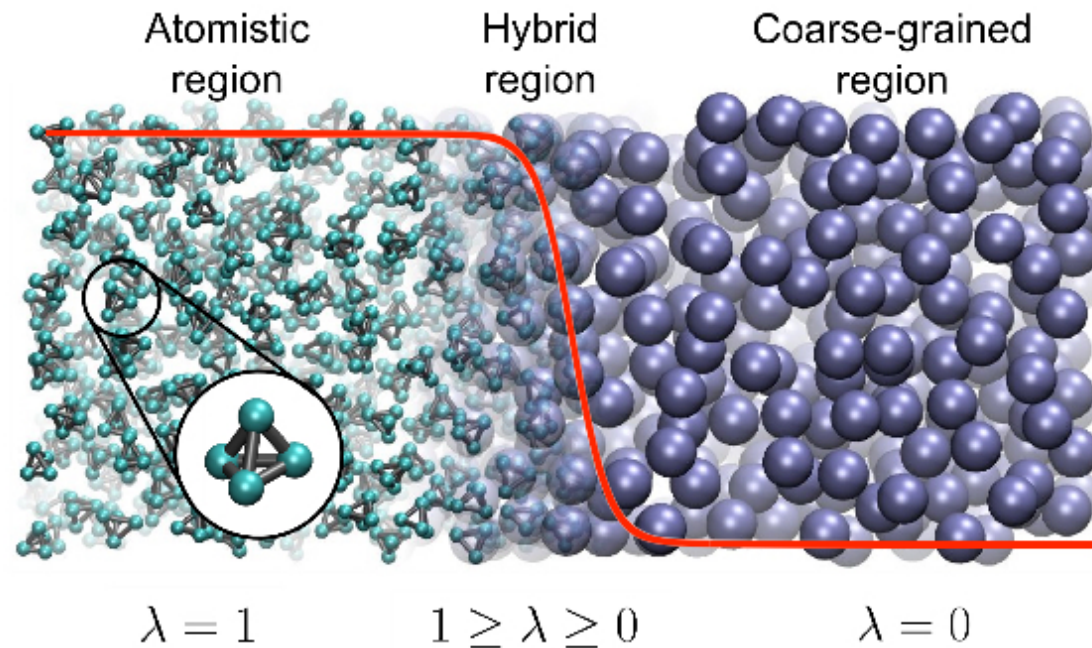
Models at different resolution are concurrently employed in different parts of the systems

AdResS

Adaptive Resolution Simulation scheme

Interpolation of the two-body force

$$\mathbf{F}_{\alpha\beta} = \lambda(\mathbf{R}_\alpha)\lambda(\mathbf{R}_\beta)\mathbf{F}_{\alpha\beta}^{AA} + (1 - \lambda(\mathbf{R}_\alpha)\lambda(\mathbf{R}_\beta))\mathbf{F}_{\alpha\beta}^{CG}$$

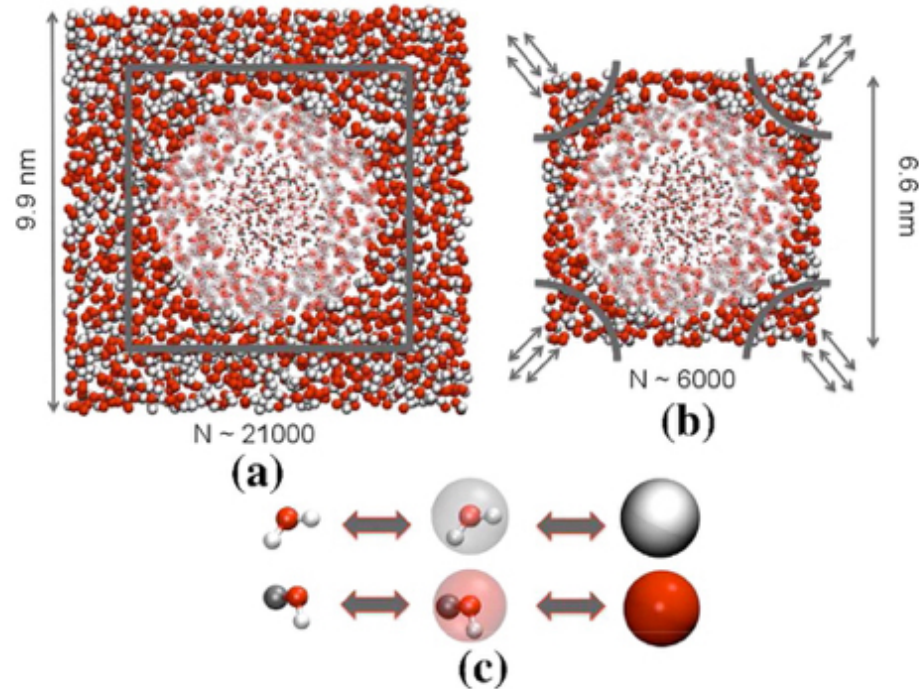
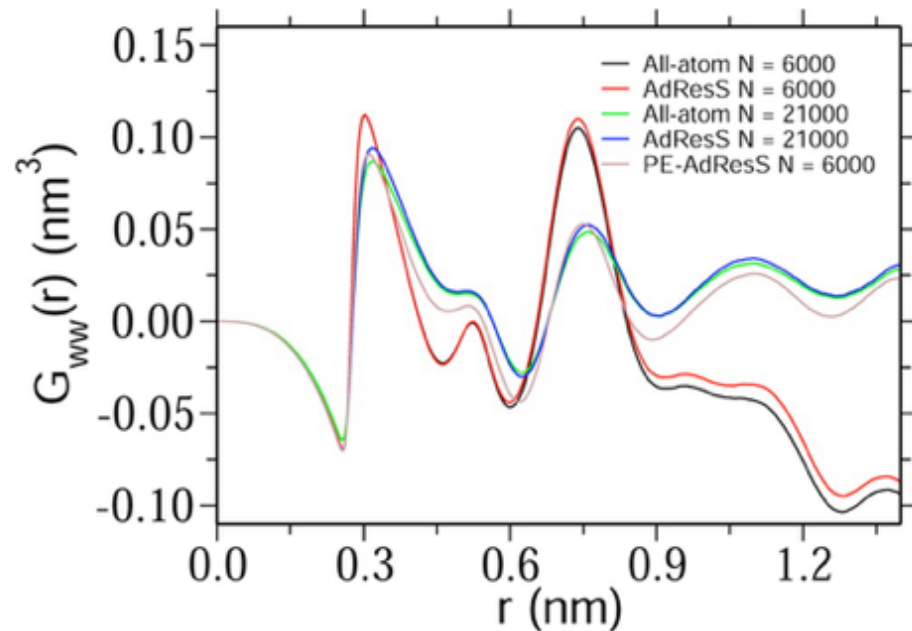


M. Praprotnik, L. Delle Site, and K. Kremer, J. Chem. Phys. 123, 2005

Quasi-Grand Canonical simulations

PNIPAm conformational transition as a function of cosolvent concentration

System size effects impact the cosolvent molecule number fluctuations



In the CG region the solvent/cosolvent identity is swapped via a Metropolis algorithm

The AA region behaves as an open system
Smaller system sizes can be employed



AdResS force-based interpolation: pros & cons

- Simplest strategy possible
- Newton's Third Law is preserved (antisymmetric force)
- No force containing derivatives of the switch function
- No Hamiltonian function exists
- A local thermostat is needed for stable simulations
- No NVE or Monte Carlo simulations
- No theory based on the partition function



AdResS force-based interpolation: pros & cons

- Simplest strategy possible
- Newton's Third Law is preserved (antisymmetric force)
- No force containing derivatives of the switch function
- No Hamiltonian function exists
- A local thermostat is needed for stable simulations
- No NVE or Monte Carlo simulations
- No theory based on the partition function

Is a Hamiltonian formulation viable?

H-AdResS

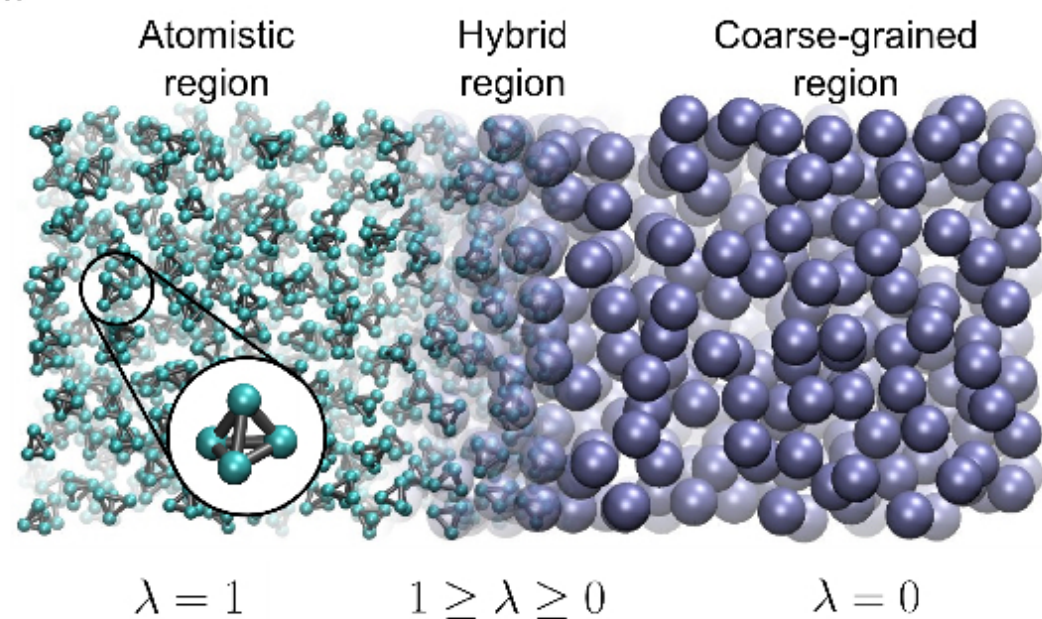
Hamiltonian Adaptive Resolution Simulation

$$H = \mathcal{K} + V^{int} + \sum_{\alpha} \{ \lambda_{\alpha} V_{\alpha}^{AA} + (1 - \lambda_{\alpha}) V_{\alpha}^{CG} \}$$

$$V_{\alpha}^{AA} \equiv \frac{1}{2} \sum_{\beta, \beta \neq \alpha}^N \sum_{ij} V^{AA}(|\mathbf{r}_{\alpha i} - \mathbf{r}_{\beta j}|)$$

$$V_{\alpha}^{CG} \equiv \frac{1}{2} \sum_{\beta, \beta \neq \alpha}^N V^{CG}(|\mathbf{R}_{\alpha} - \mathbf{R}_{\beta}|)$$

$$\lambda_{\alpha} = \lambda(\mathbf{R}_{\alpha})$$



RP, S. Fritsch, P. Español, R. Delgado-Buscalioni, K. Kremer,
R. Everaers and D. Donadio, Phys. Rev. Lett. 110, 108301 (2013)



H-AdResS

Hamiltonian Adaptive Resolution Simulation

$$H = \mathcal{K} + V^{int} + \sum_{\alpha} \{ \lambda_{\alpha} V_{\alpha}^{AA} + (1 - \lambda_{\alpha}) V_{\alpha}^{CG} \}$$

$$\begin{aligned} \mathbf{F}_{\alpha} &= \mathbf{F}_{\alpha}^{int} + \sum_{\beta, \beta \neq \alpha} \left\{ \frac{\lambda_{\alpha} + \lambda_{\beta}}{2} \mathbf{F}_{\alpha|\beta}^{AA} + \left(1 - \frac{\lambda_{\alpha} + \lambda_{\beta}}{2} \right) \mathbf{F}_{\alpha|\beta}^{CG} \right\} \\ &- [V_{\alpha}^{AA} - V_{\alpha}^{CG}] \nabla_{\alpha} \lambda_{\alpha} \end{aligned}$$

RP, S. Fritsch, P. Español, R. Delgado-Buscalioni, K. Kremer,
R. Everaers and D. Donadio, Phys. Rev. Lett. 110, 108301 (2013)



H-AdResS

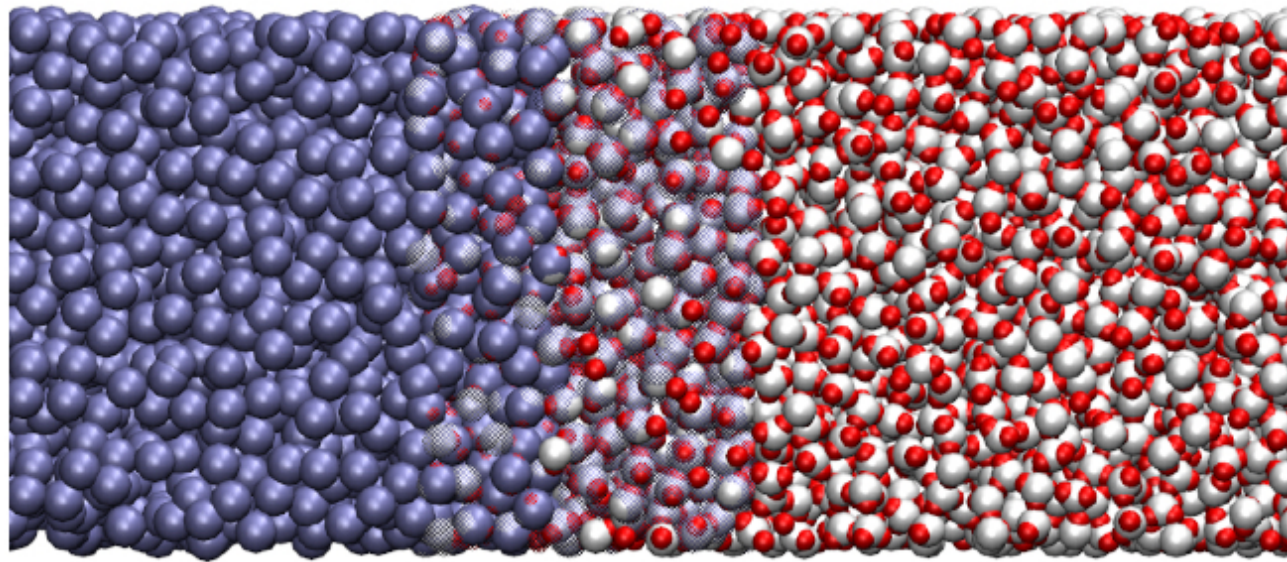
Hamiltonian Adaptive Resolution Simulation

$$H = \mathcal{K} + V^{int} + \sum_{\alpha} \left\{ \lambda_{\alpha} V_{\alpha}^{AA} + (1 - \lambda_{\alpha}) V_{\alpha}^{CG} \right\}$$

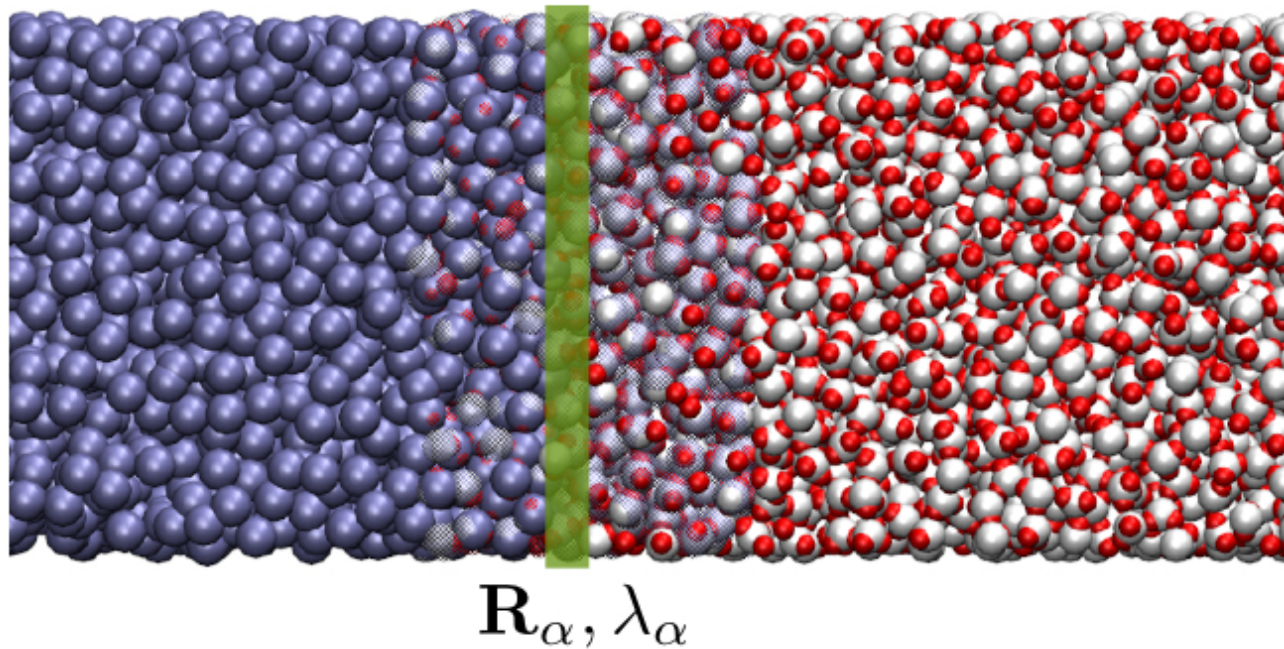
$$\begin{aligned} \mathbf{F}_{\alpha} &= \mathbf{F}_{\alpha}^{int} + \sum_{\beta, \beta \neq \alpha} \left\{ \frac{\lambda_{\alpha} + \lambda_{\beta}}{2} \mathbf{F}_{\alpha|\beta}^{AA} + \left(1 - \frac{\lambda_{\alpha} + \lambda_{\beta}}{2}\right) \mathbf{F}_{\alpha|\beta}^{CG} \right\} \\ &- [V_{\alpha}^{AA} - V_{\alpha}^{CG}] \nabla_{\alpha} \lambda_{\alpha} \end{aligned}$$

RP, S. Fritsch, P. Español, R. Delgado-Buscalioni, K. Kremer,
R. Everaers and D. Donadio, Phys. Rev. Lett. 110, 108301 (2013)

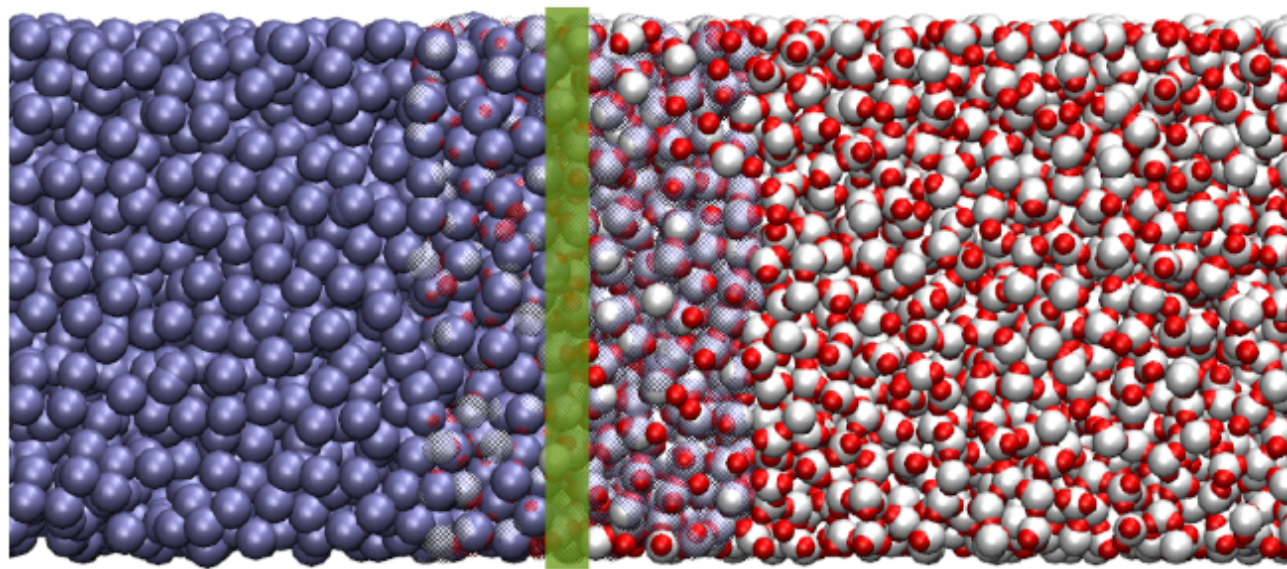
Drift force and density imbalance compensation



Drift force and density imbalance compensation



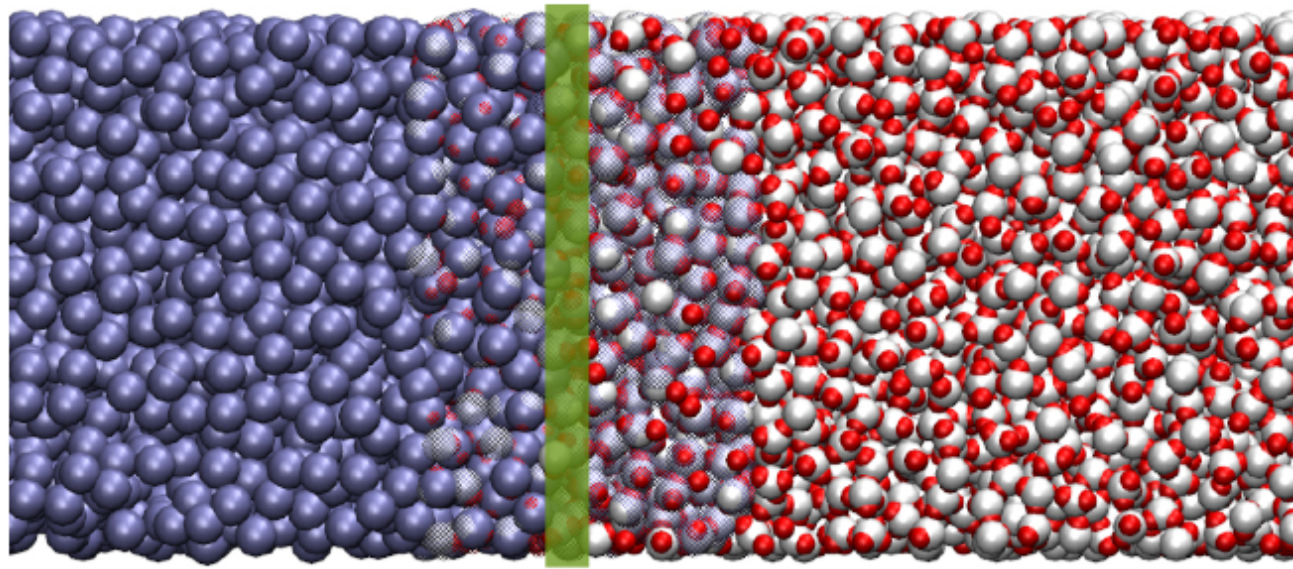
Drift force and density imbalance compensation



$\mathbf{R}_\alpha, \lambda_\alpha$

$$\langle \mathbf{F}_\alpha^\nabla \rangle = - \left\langle [V_\alpha^{AA} - V_\alpha^{CG}] \right\rangle_{\mathbf{R}_\alpha} \nabla \lambda(\mathbf{R}_\alpha)$$

Drift force and density imbalance compensation

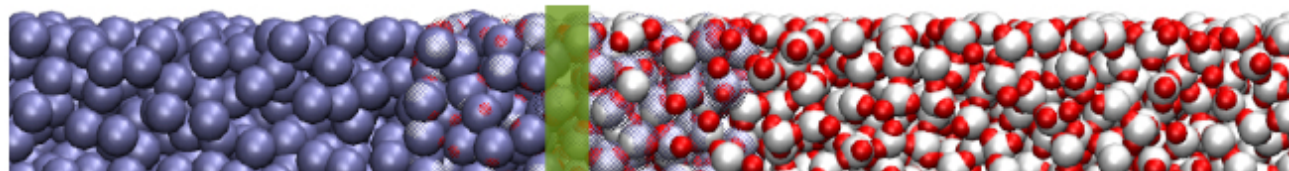


$\mathbf{R}_\alpha, \lambda_\alpha$

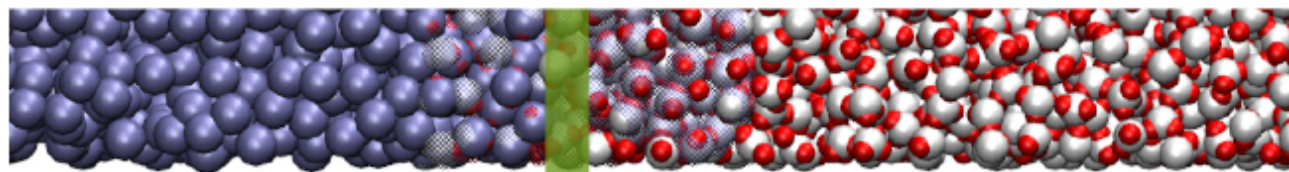
$$\langle \mathbf{F}_\alpha^\nabla \rangle = - \left\langle [V_\alpha^{AA} - V_\alpha^{CG}] \right\rangle_{\mathbf{R}_\alpha} \nabla \lambda(\mathbf{R}_\alpha)$$

$$\left\langle [V_\alpha^{AA} - V_\alpha^{CG}] \right\rangle_{\mathbf{R}_\alpha} \simeq \frac{1}{N} \frac{dF(\lambda)}{d\lambda}$$

Drift force and density imbalance compensation



The force in the hybrid region is proportional
to the gradient of Helmholtz free energy
as a function of the resolution



$\mathbf{R}_\alpha, \lambda_\alpha$

$$\langle \mathbf{F}_\alpha^\nabla \rangle = - \langle [V_\alpha^{AA} - V_\alpha^{CG}] \rangle_{\mathbf{R}_\alpha} \nabla \lambda(\mathbf{R}_\alpha)$$

$$\langle [V_\alpha^{AA} - V_\alpha^{CG}] \rangle_{\mathbf{R}_\alpha} \simeq \frac{1}{N} \frac{dF(\lambda)}{d\lambda}$$

Drift force and density imbalance compensation

Modify the Hamiltonian introducing a compensation term

$$H_{\Delta} = H - \sum_{\alpha=1}^N \Delta H(\lambda(\mathbf{R}_{\alpha}))$$

$$\langle [V_{\alpha}^{AA} - V_{\alpha}^{CG}] \rangle_{\mathbf{R}_{\alpha}} \simeq \frac{1}{N} \frac{dF(\lambda)}{d\lambda}$$

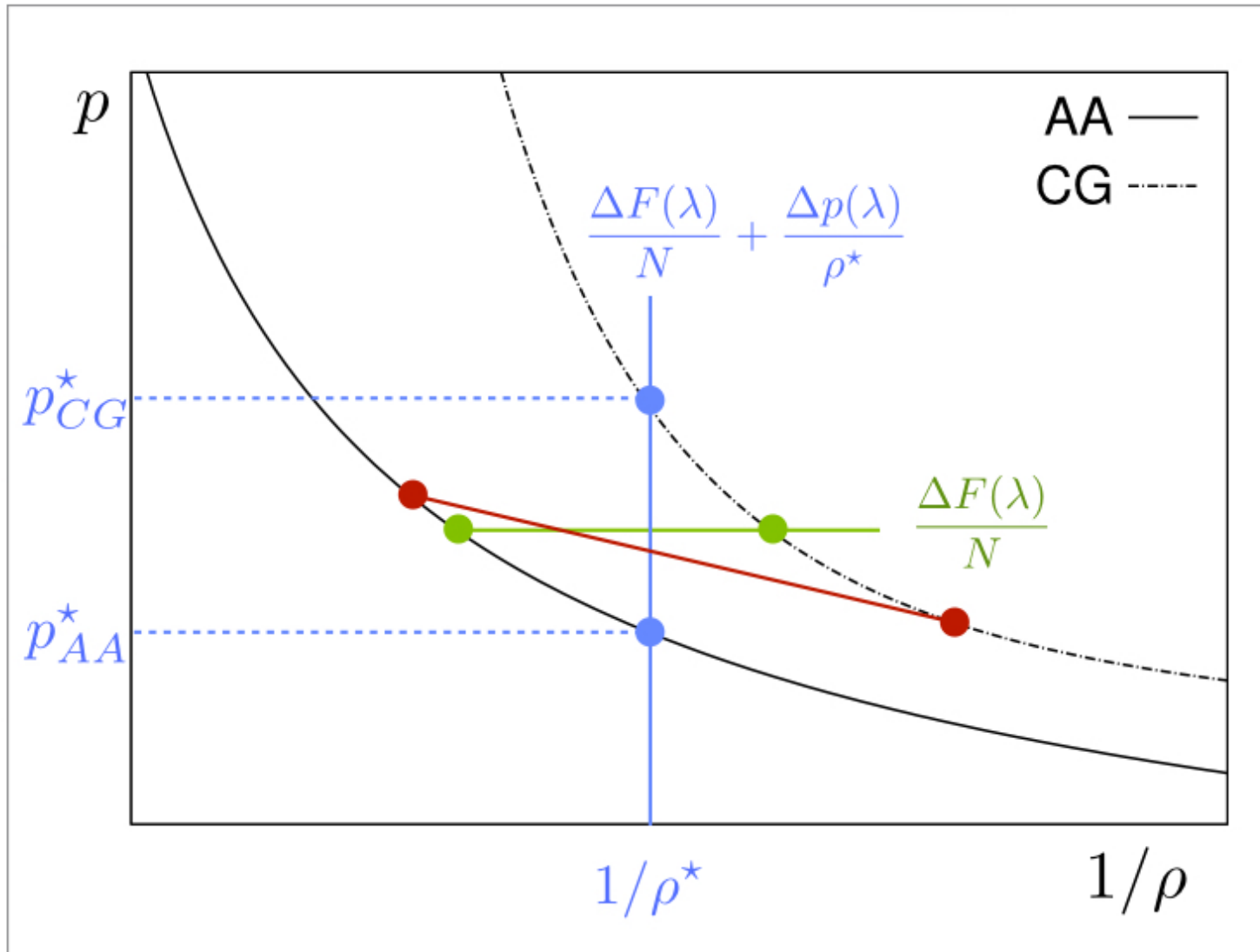
$$\Delta H(\lambda) \equiv \frac{\Delta F(\lambda)}{N}$$

Helmholtz free energy cancels the drift force in the hybrid region

Gibbs free energy removes also the density imbalance between AA and CG

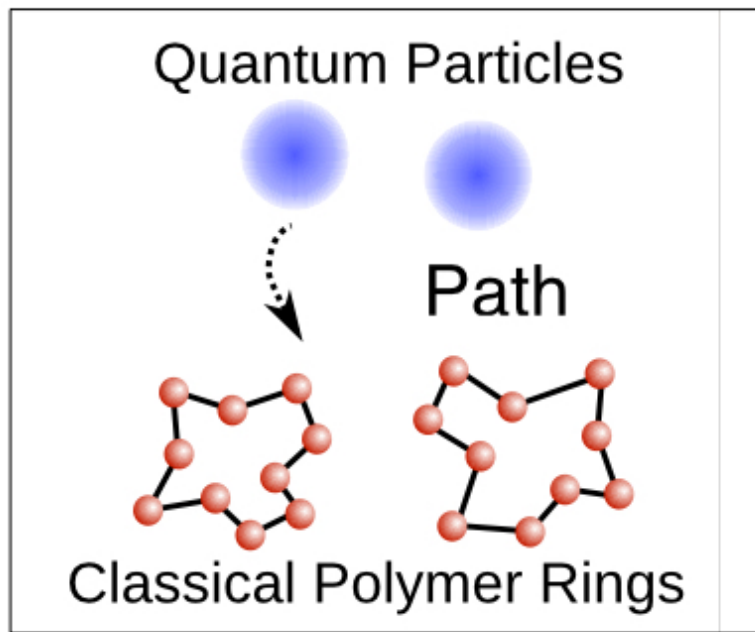
$$\Delta H(\lambda) \equiv \Delta \mu(\lambda) = \frac{\Delta F(\lambda)}{N} + \frac{\Delta p(\lambda)}{\rho^*}$$

H-AdResS: the big picture



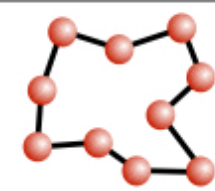
RP, S. Fritsch, P. Español, R. Delgado-Buscalioni, K. Kremer,
R. Everaers and D. Donadio, Phys. Rev. Lett. 110, 108301 (2013)

H-AdResS Quantum/Classical coupling



$$m \rightarrow \mu(\lambda) = \lambda m + (1 - \lambda)M$$

$$\mu(\lambda = 1) = m$$



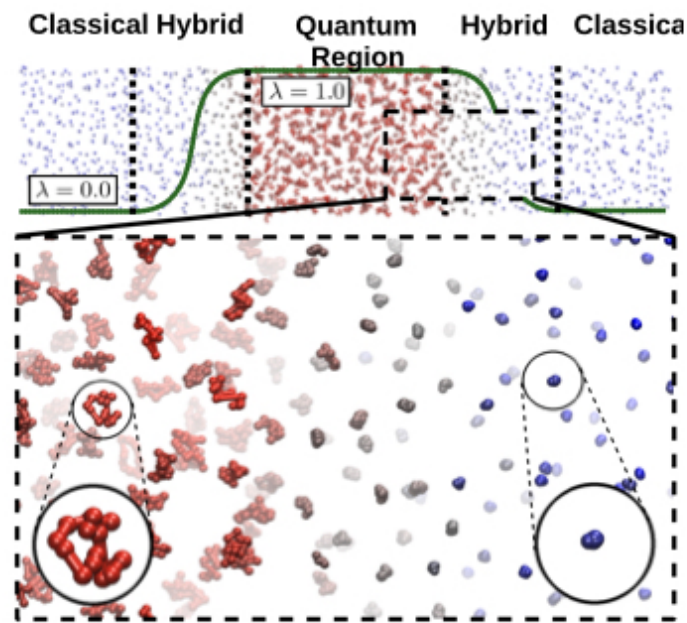
$$\mu(\lambda = 0) = M$$



$$V_P^\mu = \sum_{l=1}^P \sum_{\alpha=1}^N \left\{ \frac{\mu_{\alpha,l} \omega_P^2}{2} |\mathbf{r}_{\alpha,l} - \mathbf{r}_{\alpha,l+1}|^2 - \frac{3}{2\beta} \log \frac{\mu_{\alpha,l}}{m} \right. \\ \left. + \frac{1}{P} [\lambda_{\alpha,l} V_{\alpha,l}^1 + (1 - \lambda_{\alpha,l}) V_{\alpha,l}^0 - \Delta H(\lambda_{\alpha,l})] \right\}$$

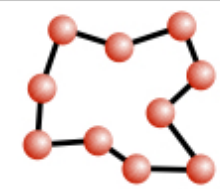
K. Kreis, M. E. Tuckerman, D. Donadio, K. Kremer and RP, JCTC (2016)
 K. Kreis, K. Kremer, RP, M. E. Tuckerman, JCP (2017)

H-AdResS Quantum/Classical coupling



$$m \rightarrow \mu(\lambda) = \lambda m + (1 - \lambda)M$$

$$\mu(\lambda = 1) = m$$



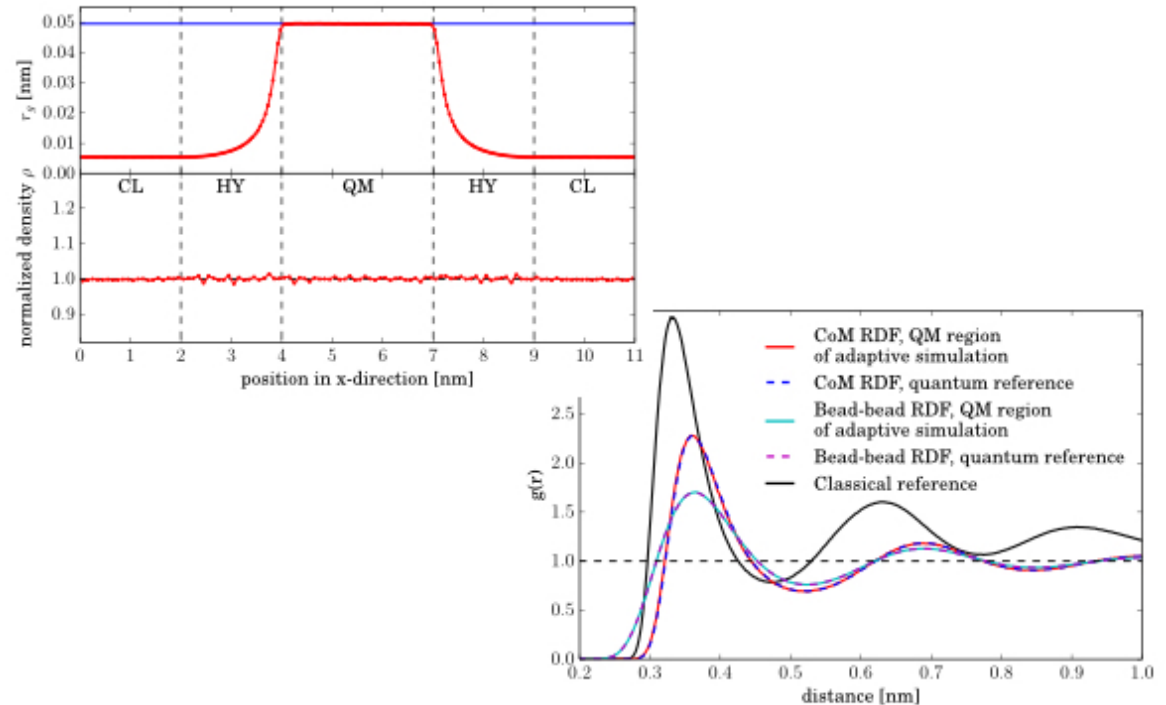
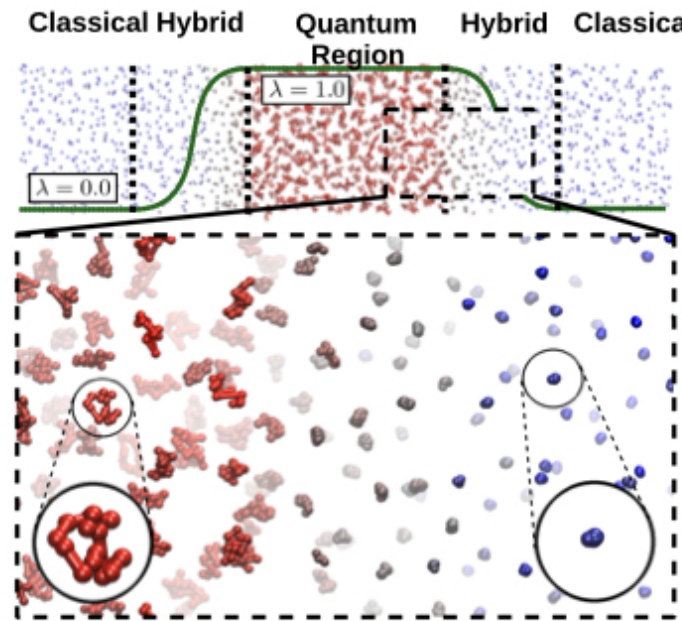
$$\mu(\lambda = 0) = M$$



$$V_P^\mu = \sum_{l=1}^P \sum_{\alpha=1}^N \left\{ \frac{\mu_{\alpha,l} \omega_P^2}{2} |\mathbf{r}_{\alpha,l} - \mathbf{r}_{\alpha,l+1}|^2 - \frac{3}{2\beta} \log \frac{\mu_{\alpha,l}}{m} \right. \\ \left. + \frac{1}{P} [\lambda_{\alpha,l} V_{\alpha,l}^1 + (1 - \lambda_{\alpha,l}) V_{\alpha,l}^0 - \Delta H(\lambda_{\alpha,l})] \right\}$$

K. Kreis, M. E. Tuckerman, D. Donadio, K. Kremer and RP, JCTC (2016)
 K. Kreis, K. Kremer, RP, M. E. Tuckerman, JCP (2017)

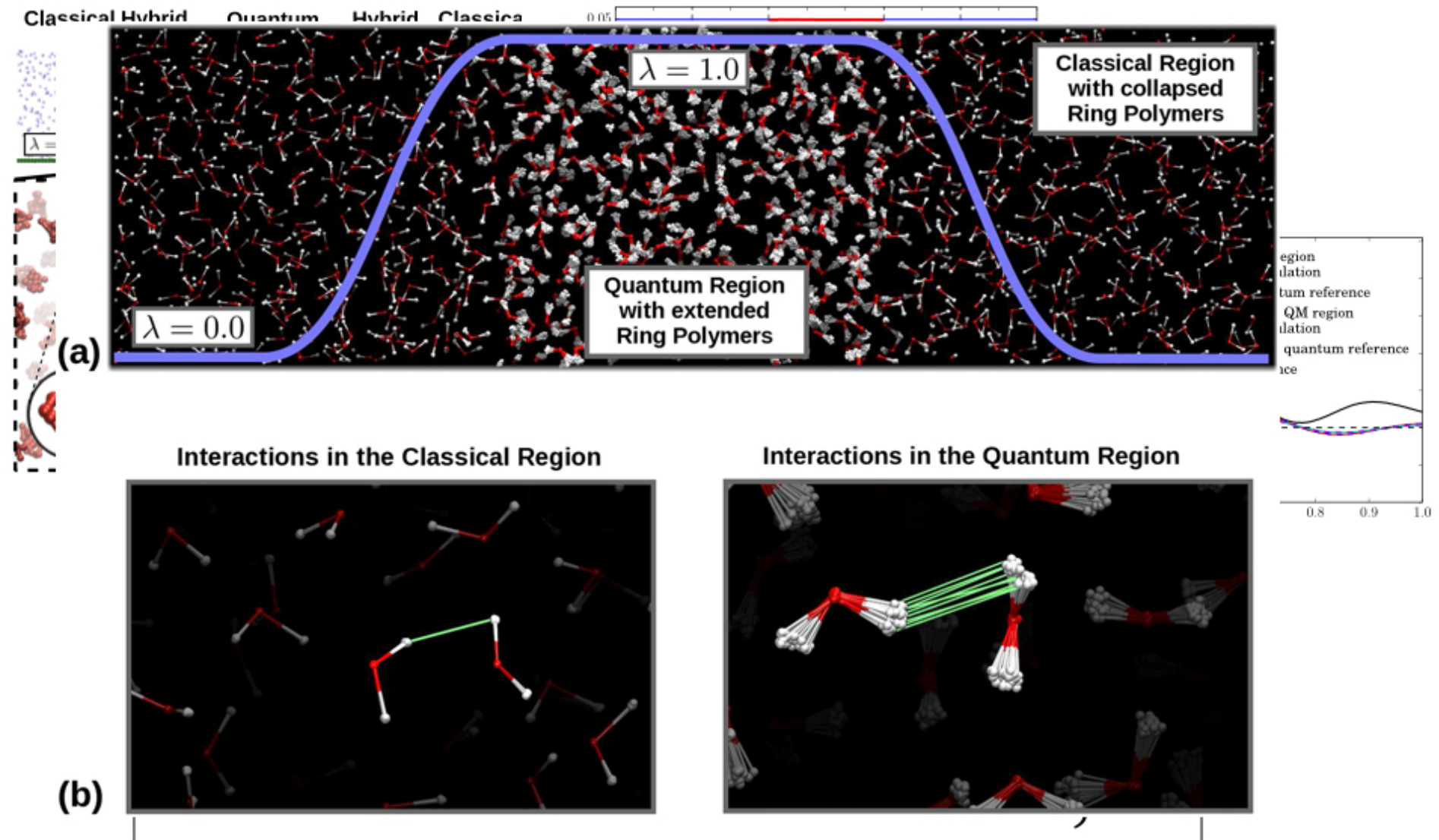
H-AdResS Quantum/Classical coupling



$$V_P^\mu = \sum_{l=1}^P \sum_{\alpha=1}^N \left\{ \frac{\mu_{\alpha,l} \omega_P^2}{2} |\mathbf{r}_{\alpha,l} - \mathbf{r}_{\alpha,l+1}|^2 - \frac{3}{2\beta} \log \frac{\mu_{\alpha,l}}{m} \right. \\ \left. + \frac{1}{P} [\lambda_{\alpha,l} V_{\alpha,l}^1 + (1 - \lambda_{\alpha,l}) V_{\alpha,l}^0 - \Delta H(\lambda_{\alpha,l})] \right\}$$

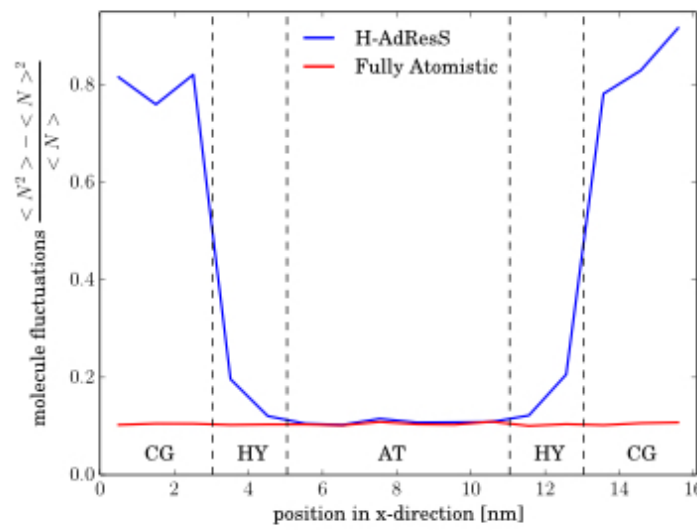
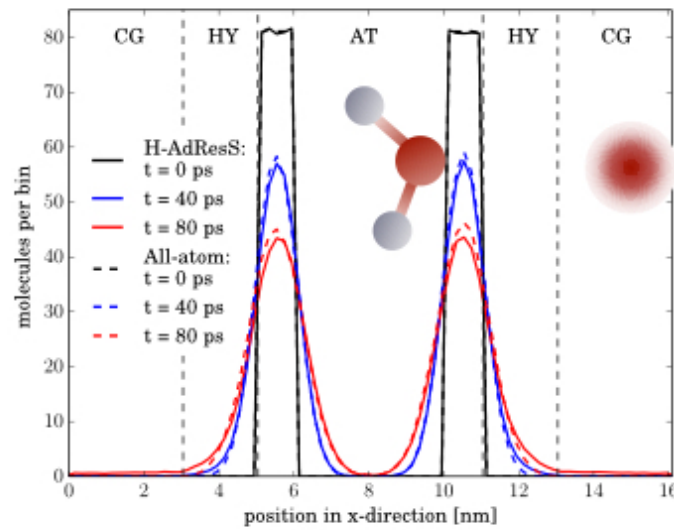
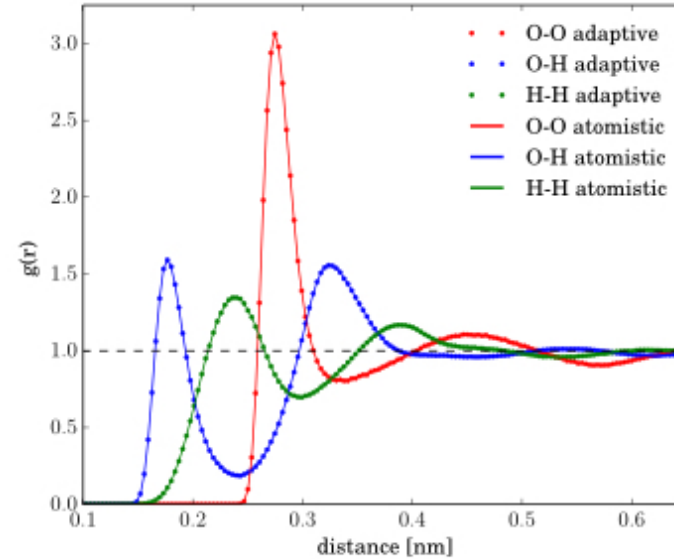
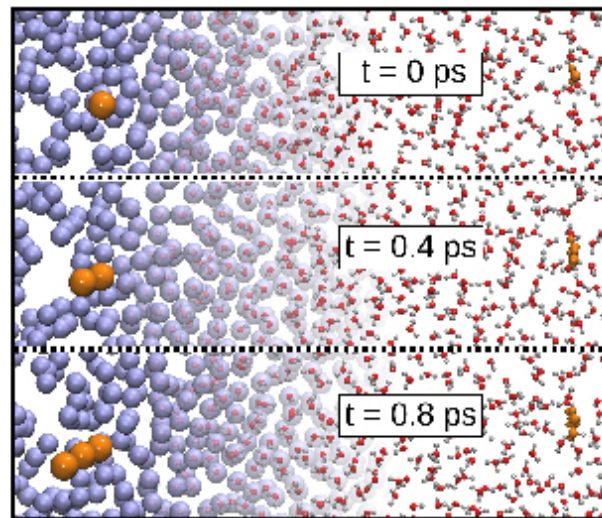
K. Kreis, M. E. Tuckerman, D. Donadio, K. Kremer and RP, JCTC (2016)
 K. Kreis, K. Kremer, RP, M. E. Tuckerman, JCP (2017)

H-AdResS Quantum/Classical coupling

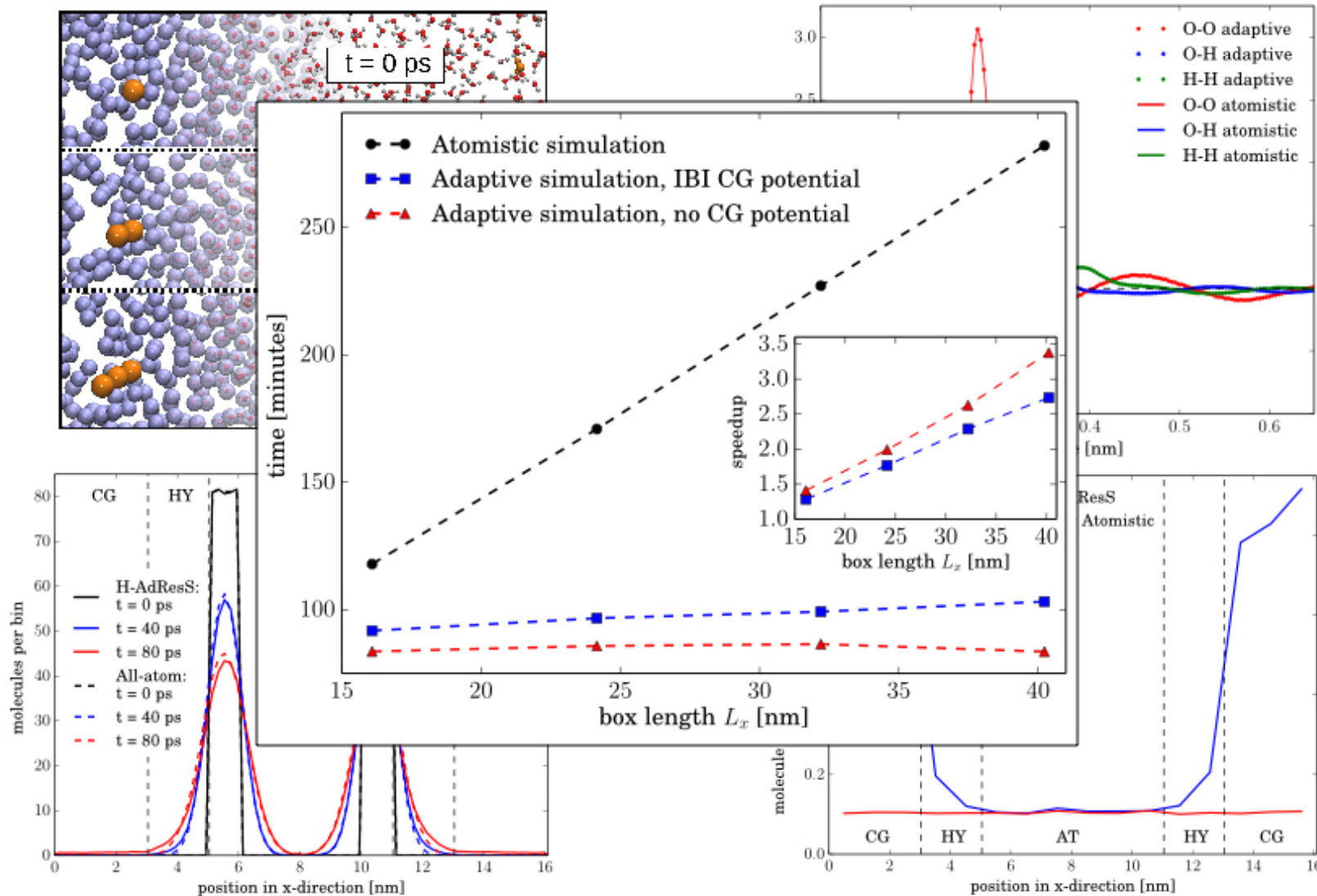


K. Kreis, M. E. Tuckerman, D. Donadio, K. Kremer and RP, JCTC (2016)
 K. Kreis, K. Kremer, RP, M. E. Tuckerman, JCP (2017)

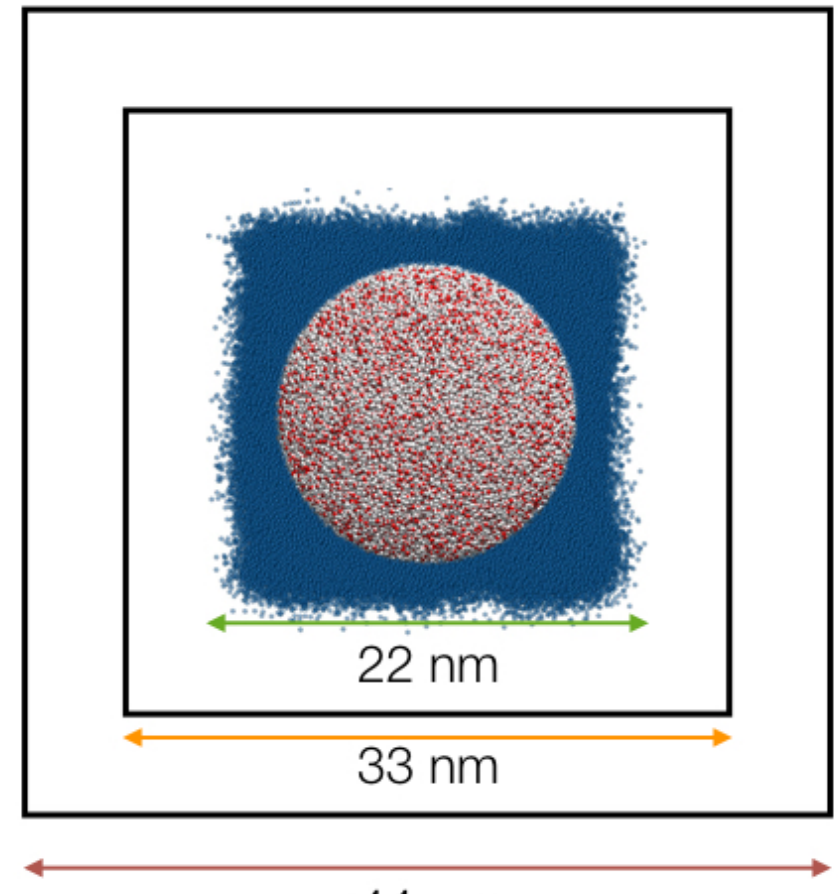
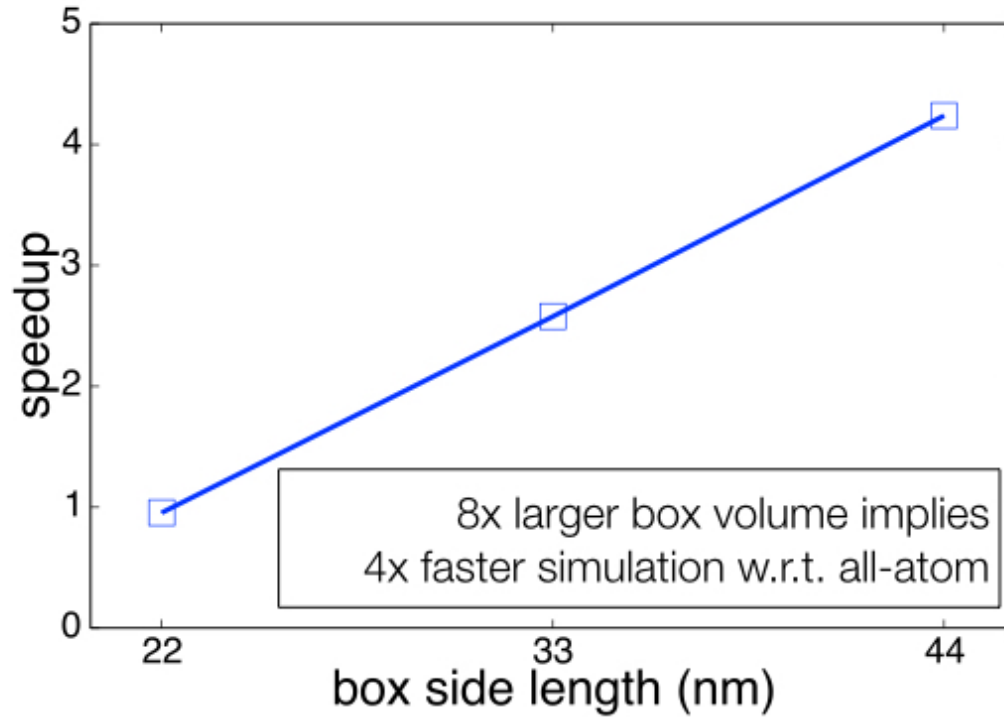
H-AdResS water/ideal gas coupling



H-AdResS water/ideal gas coupling



Coupling all-atom and ideal gas models

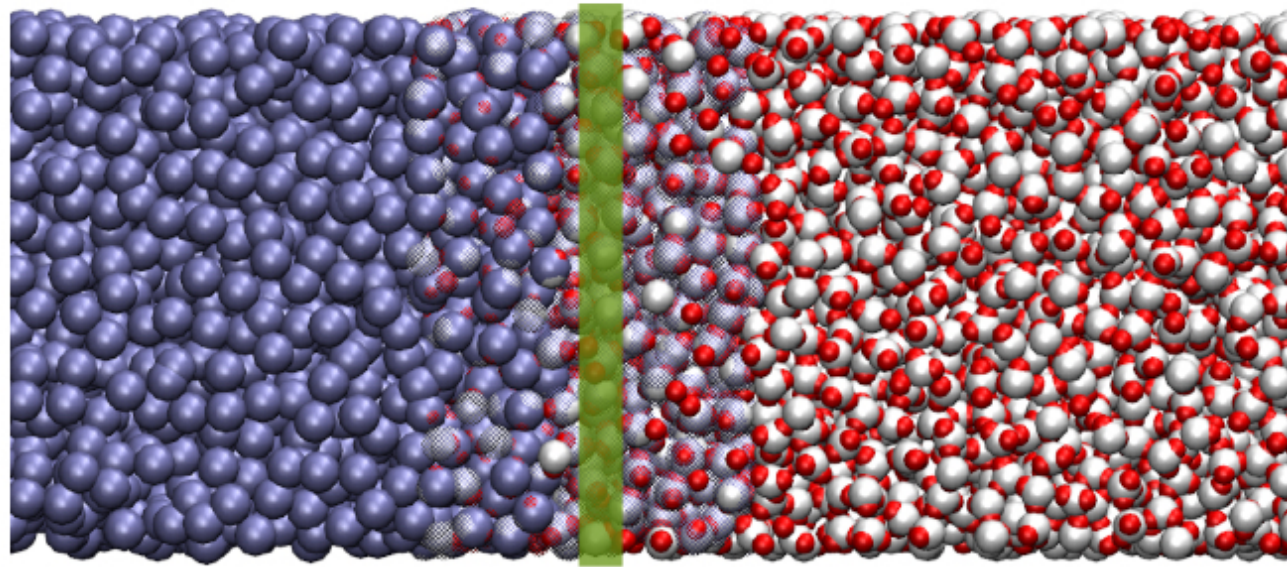


System setup

- Water in cubic box
- H-AdResS adaptive resolution simulation
- All-atom SPC/E water model coupled to ideal gas
- Spherical atomistic region of 9 nm radius (*kept fixed*)
- Box side of 22, 33, 44 nm (reps. 902286, 3090900, 7218309 atoms)
- 1000 time steps ($dt = 1$ fs)
- Single core runs on Intel(R) Core(TM) i5-4690 CPU @ 3.50GHz
- Spherical atomistic region size compatible with solvated STMV viral capsid

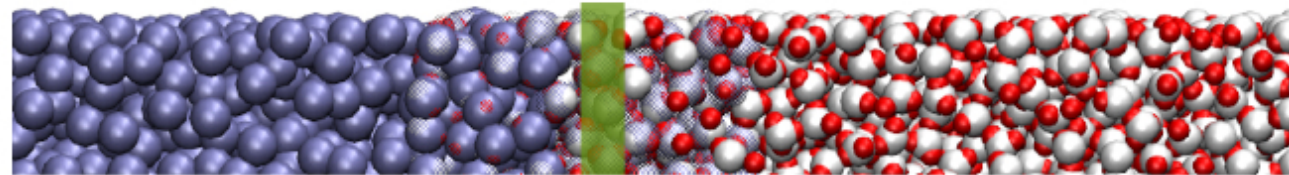
Simulations by M. Heidari, MPIP

Dual-res simulations for chemical physics

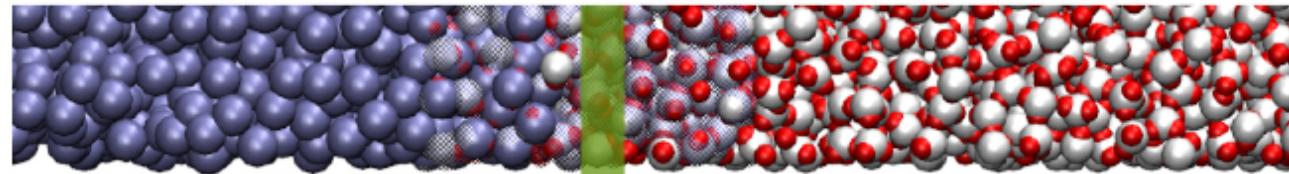


$$\mathbf{R}_\alpha, \lambda_\alpha$$

Dual-res simulations for chemical physics

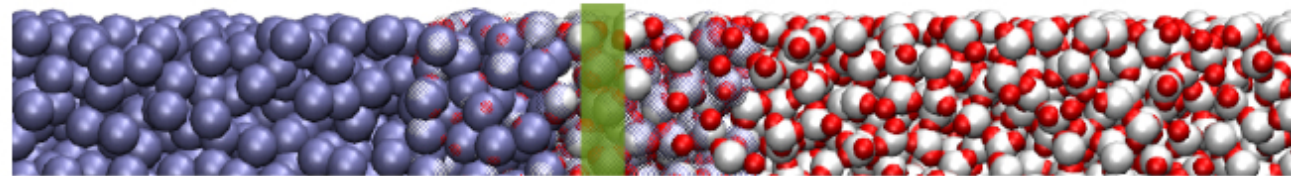


The drift force in the hybrid region
pushes molecules where the free energy is lower

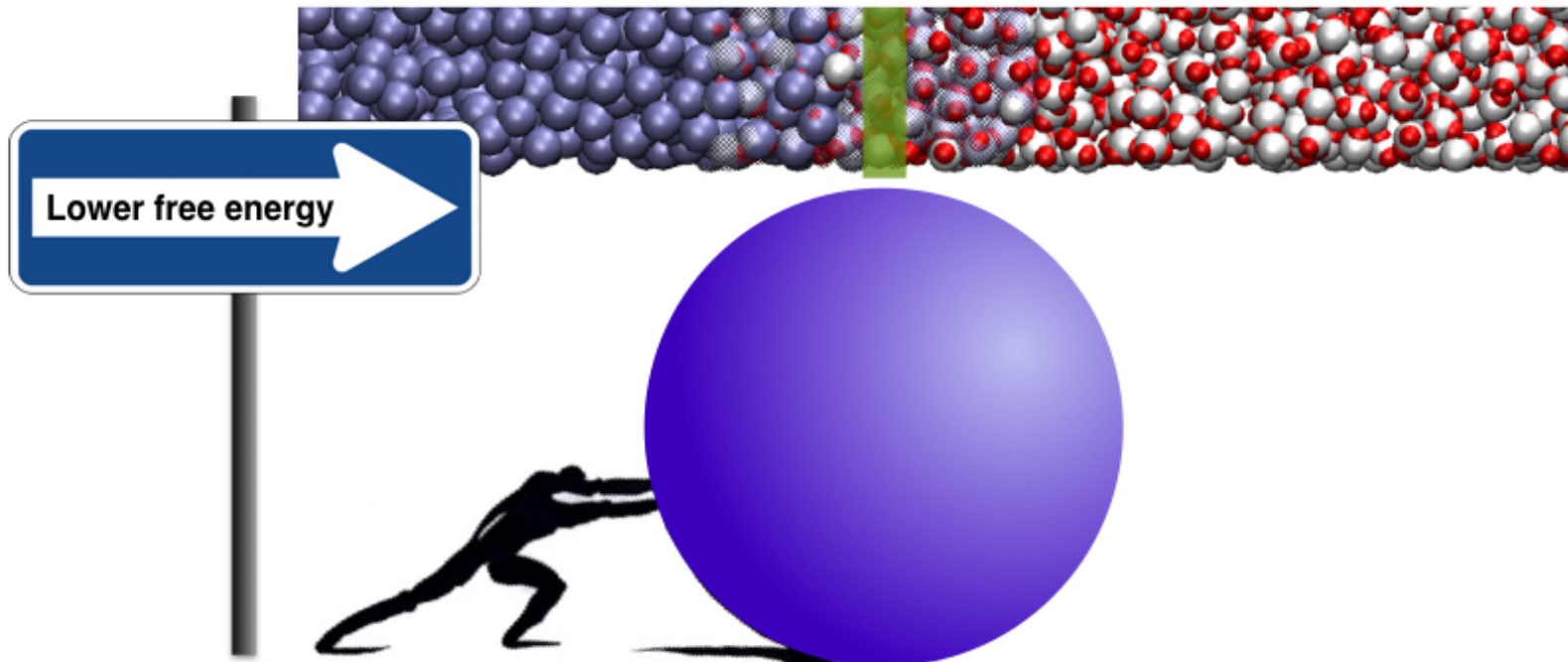


$$\mathbf{R}_\alpha, \lambda_\alpha$$

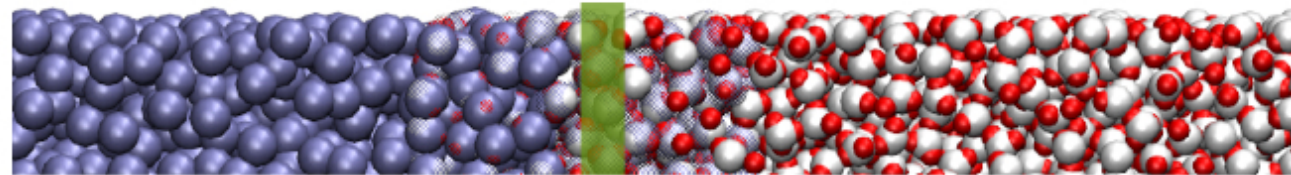
Dual-res simulations for chemical physics



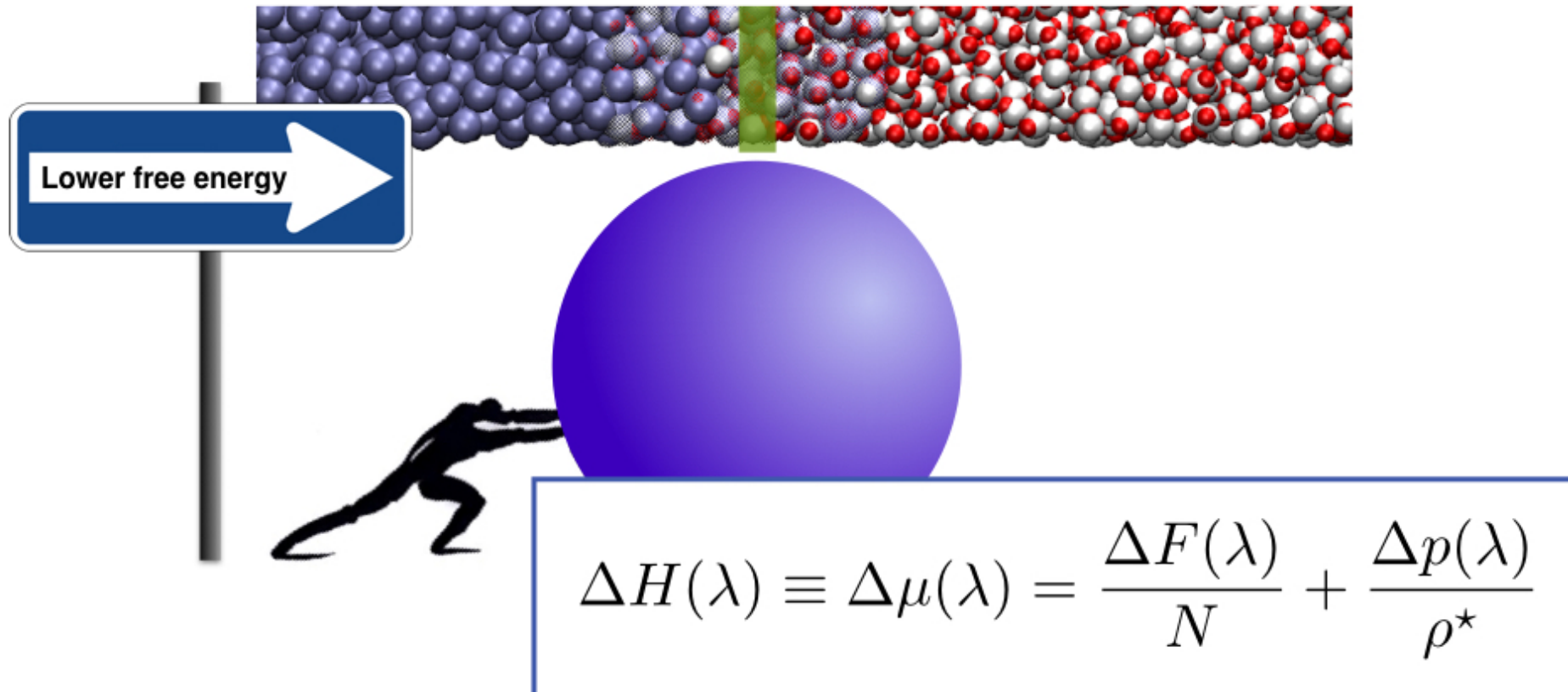
The drift force in the hybrid region
pushes molecules where the free energy is lower



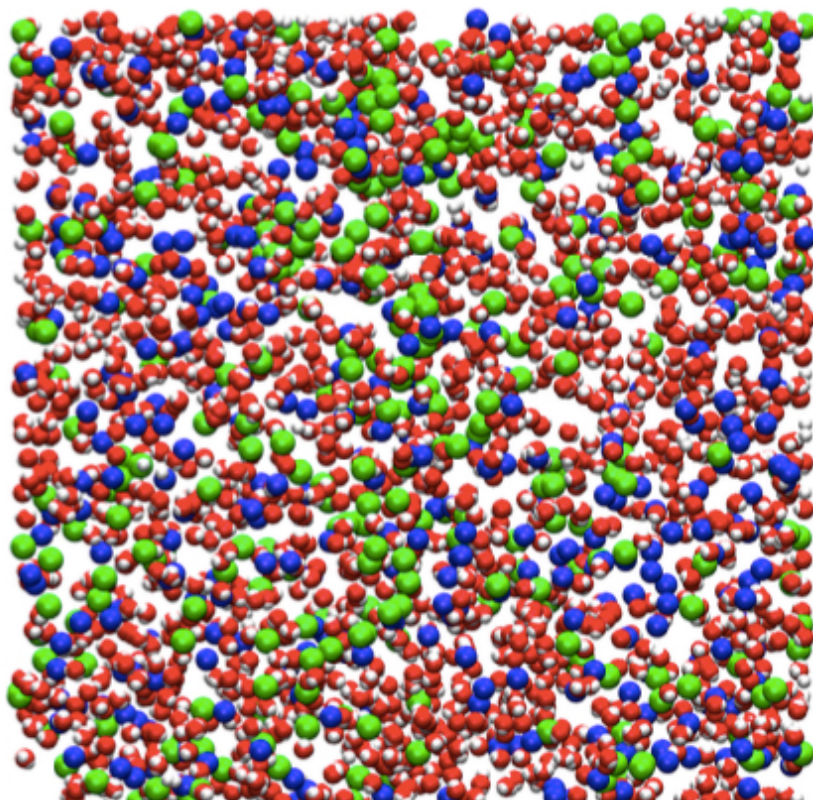
Dual-res simulations for chemical physics



The drift force in the hybrid region
pushes molecules where the free energy is lower

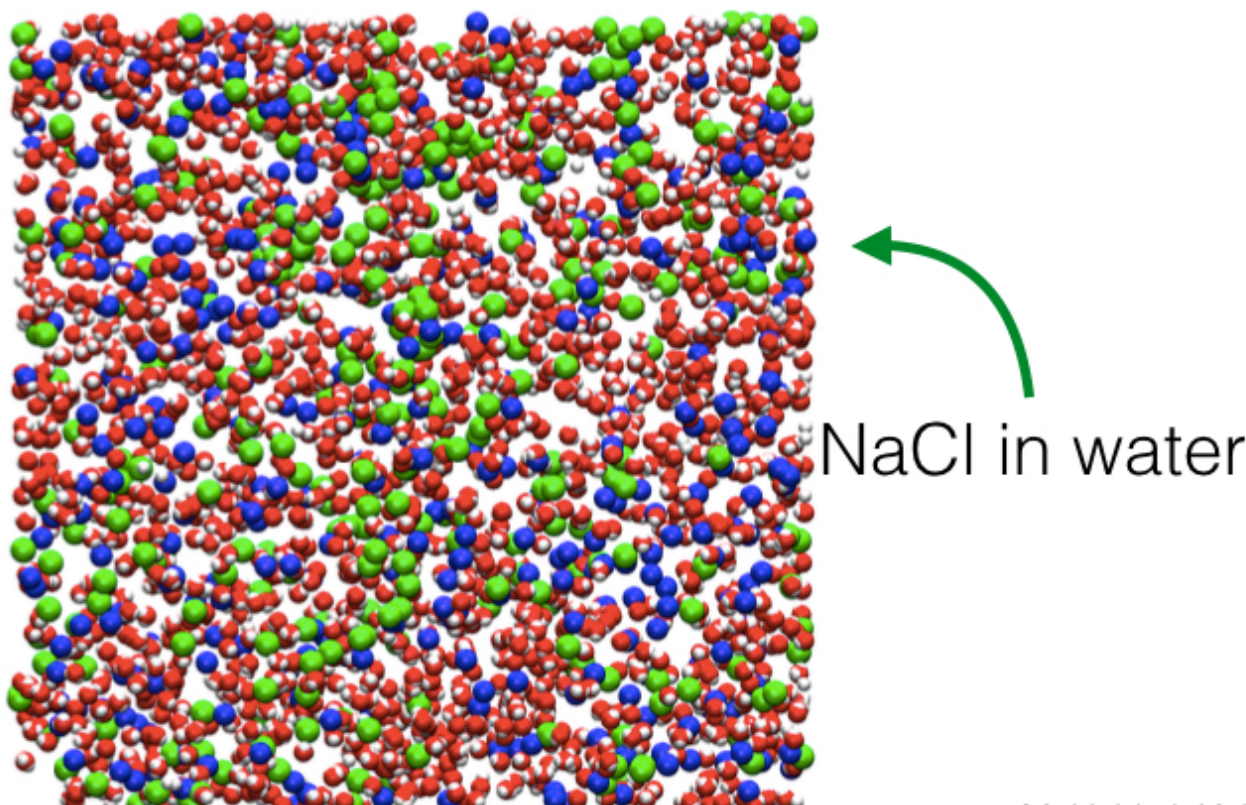


Fast calculation of chemical potentials



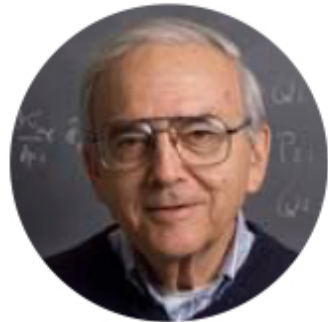
M. Heidari, K. Kremer, R. Cortes-Huerto and RP, submitted

Fast calculation of chemical potentials

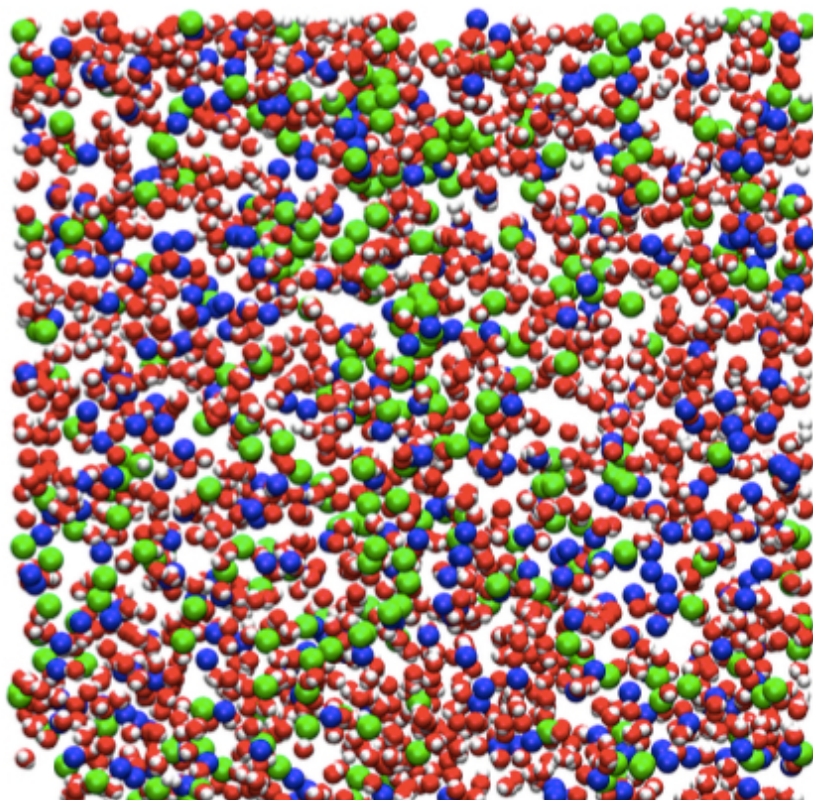


M. Heidari, K. Kremer, R. Cortes-Huerto and RP, submitted

Fast calculation of chemical potentials



Ben Widom



NaCl in water

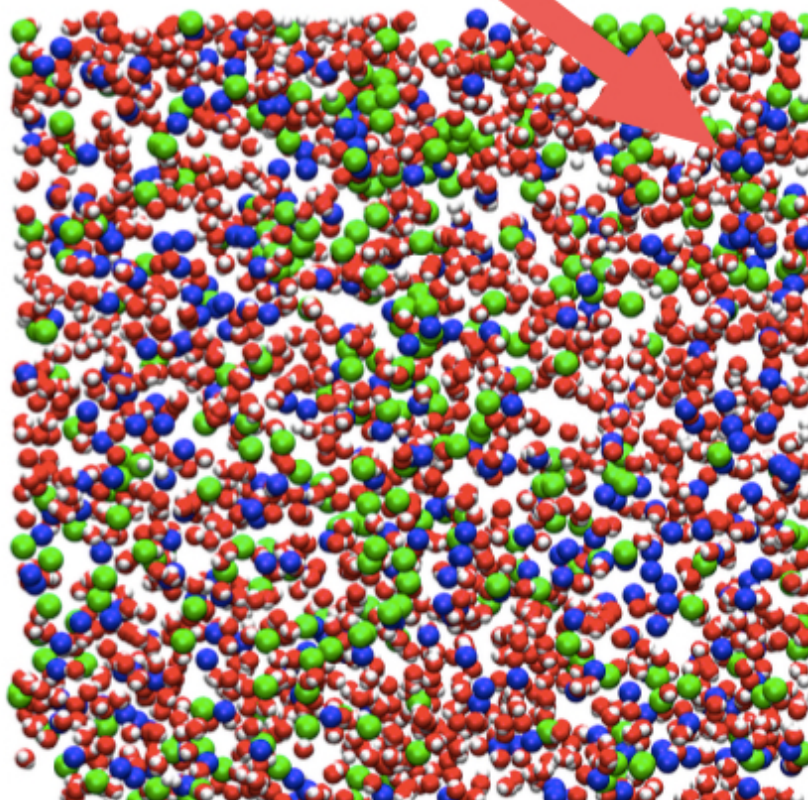


M. Heidari, K. Kremer, R. Cortes-Huerto and RP, submitted

Fast calculation of chemical potentials



Ben Widom



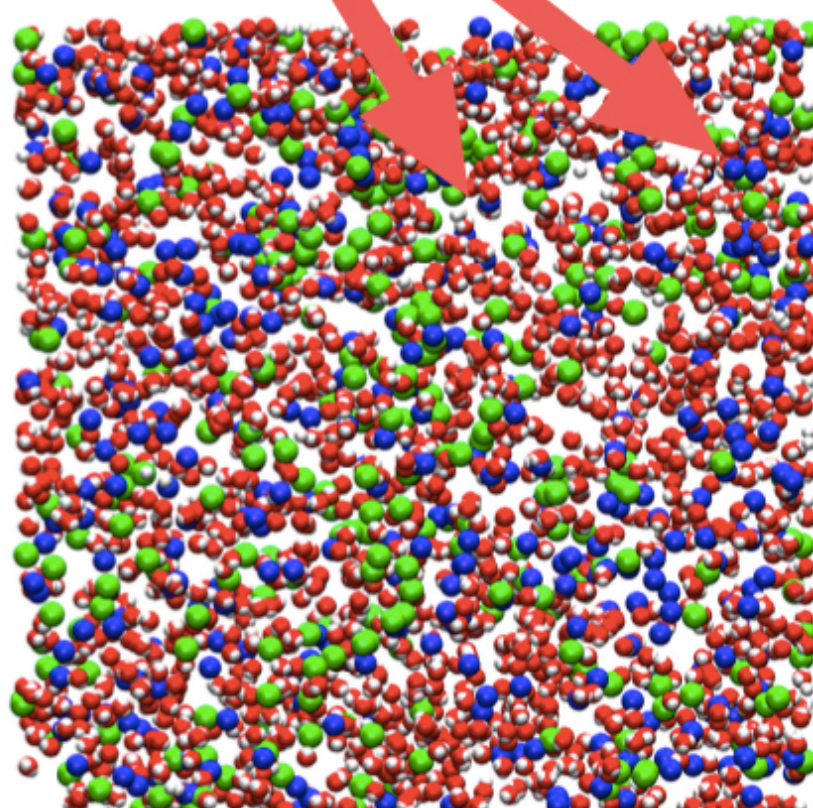
NaCl in water

M. Heidari, K. Kremer, R. Cortes-Huerto and RP, submitted

Fast calculation of chemical potentials



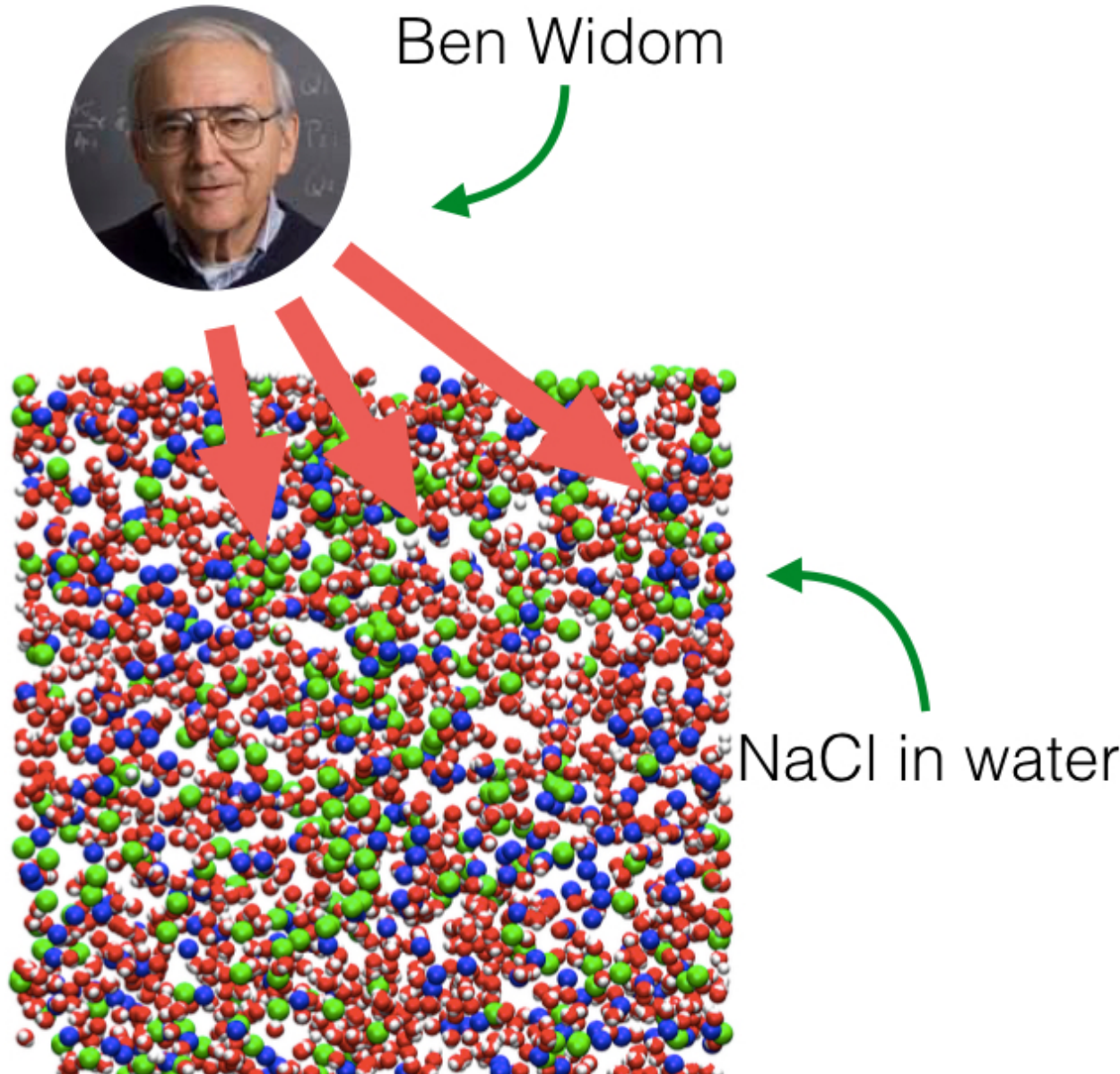
Ben Widom



NaCl in water

M. Heidari, K. Kremer, R. Cortes-Huerto and RP, submitted

Fast calculation of chemical potentials

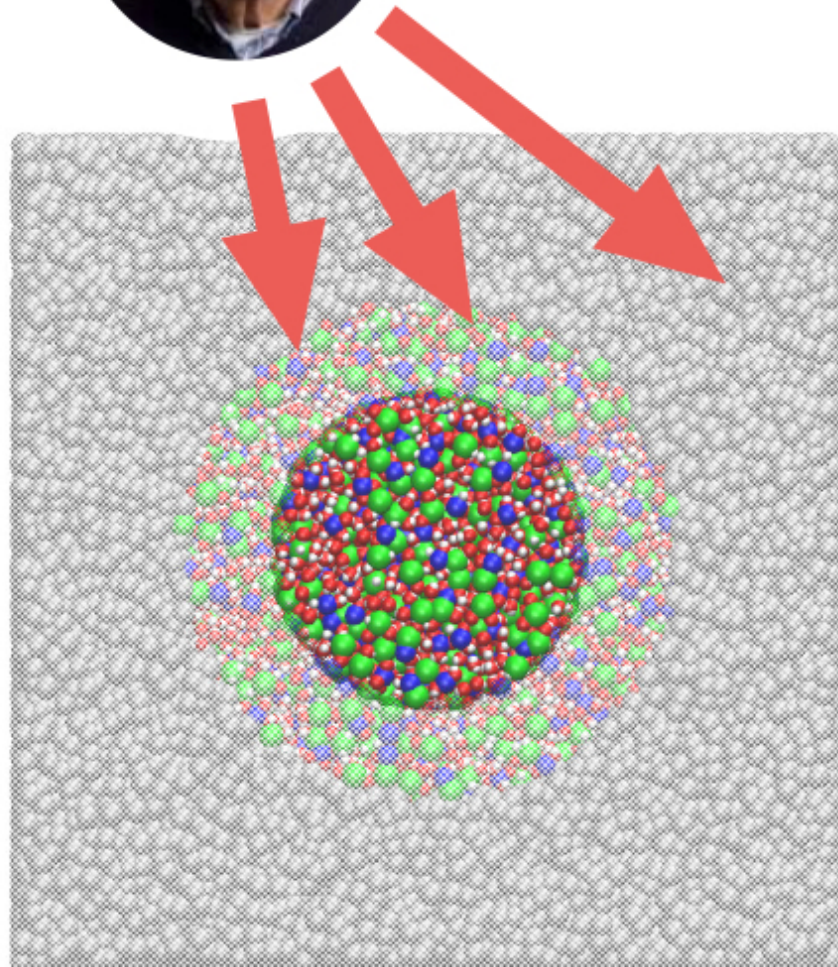


M. Heidari, K. Kremer, R. Cortes-Huerto and RP, submitted

Fast calculation of chemical potentials

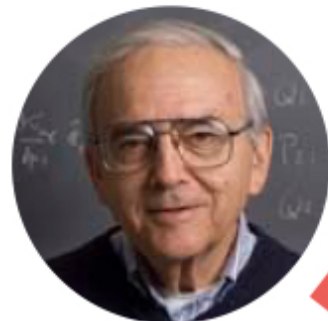


Ben Widom

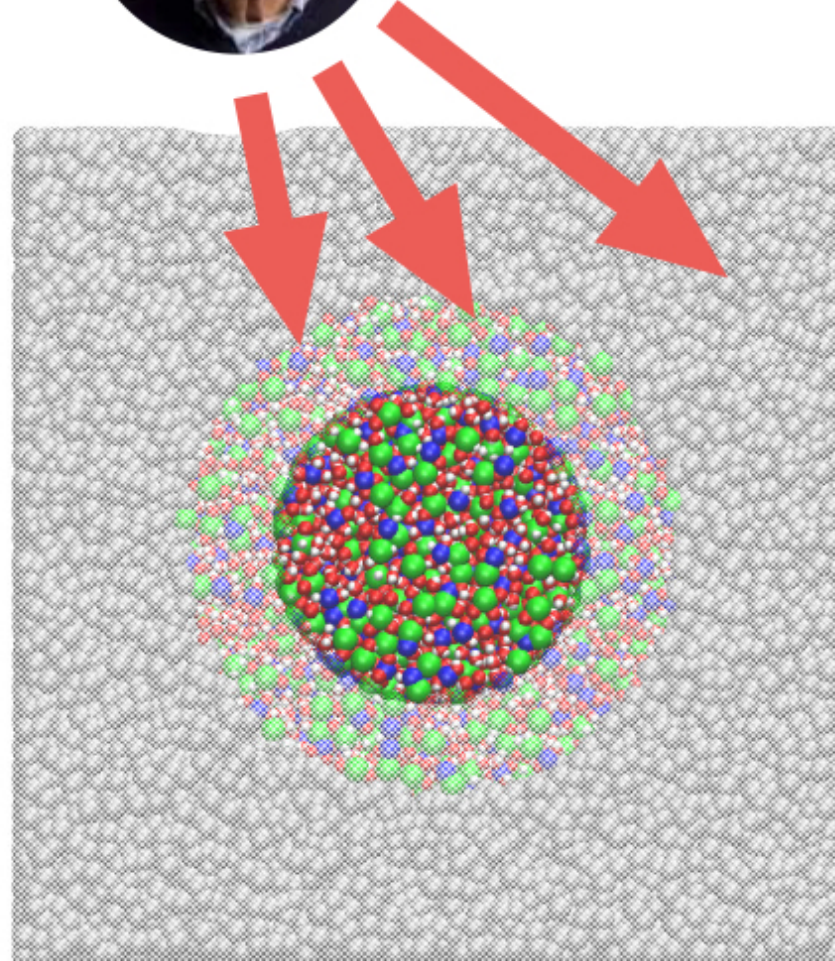


M. Heidari, K. Kremer, R. Cortes-Huerto and RP, submitted

Fast calculation of chemical potentials



Ben Widom

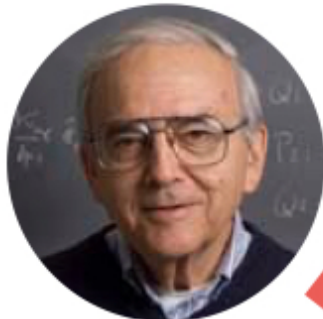


The FEC is the chemical potential difference between high and low resolution model

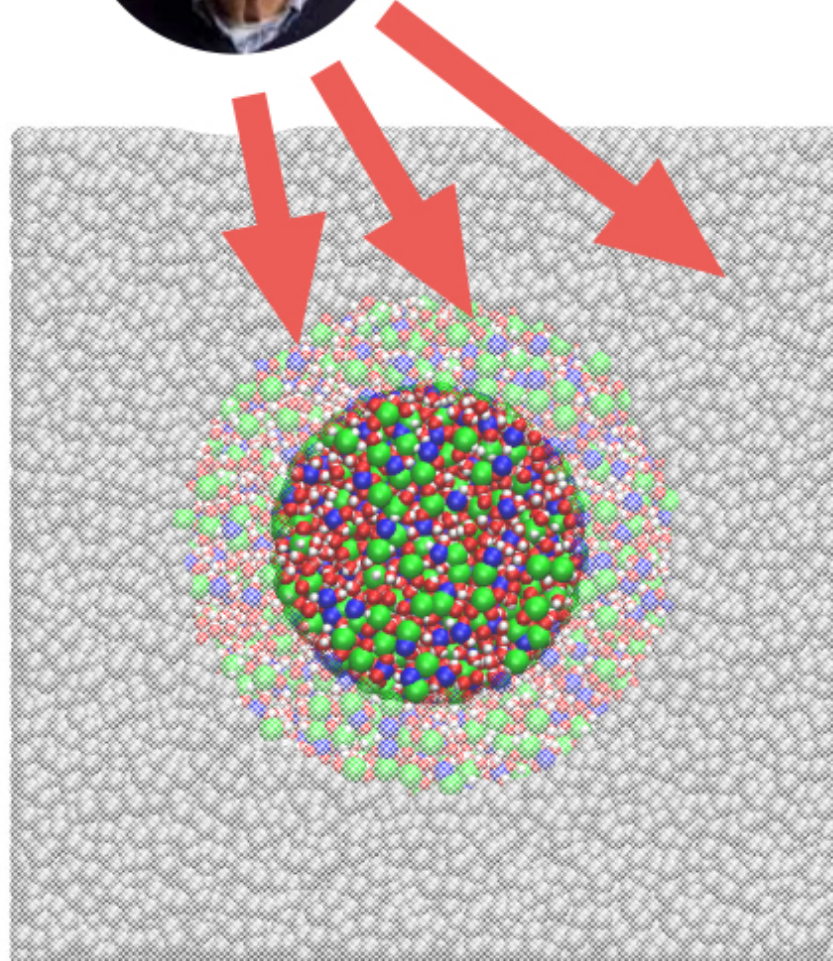
**If the CG model is an ideal gas,
the FEC equates the excess chemical potential**

M. Heidari, K. Kremer, R. Cortes-Huerto and RP, submitted

Fast calculation of chemical potentials

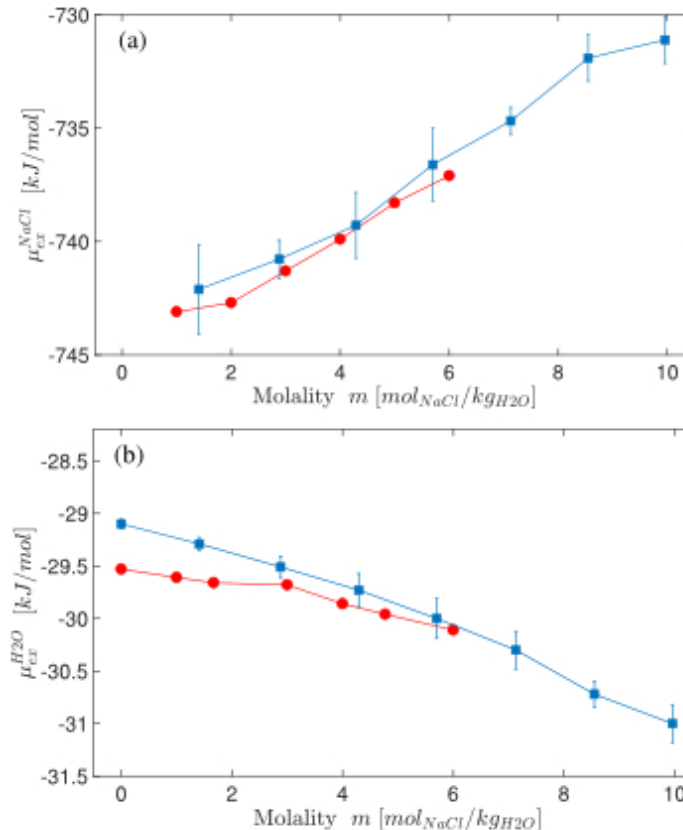


Ben Widom



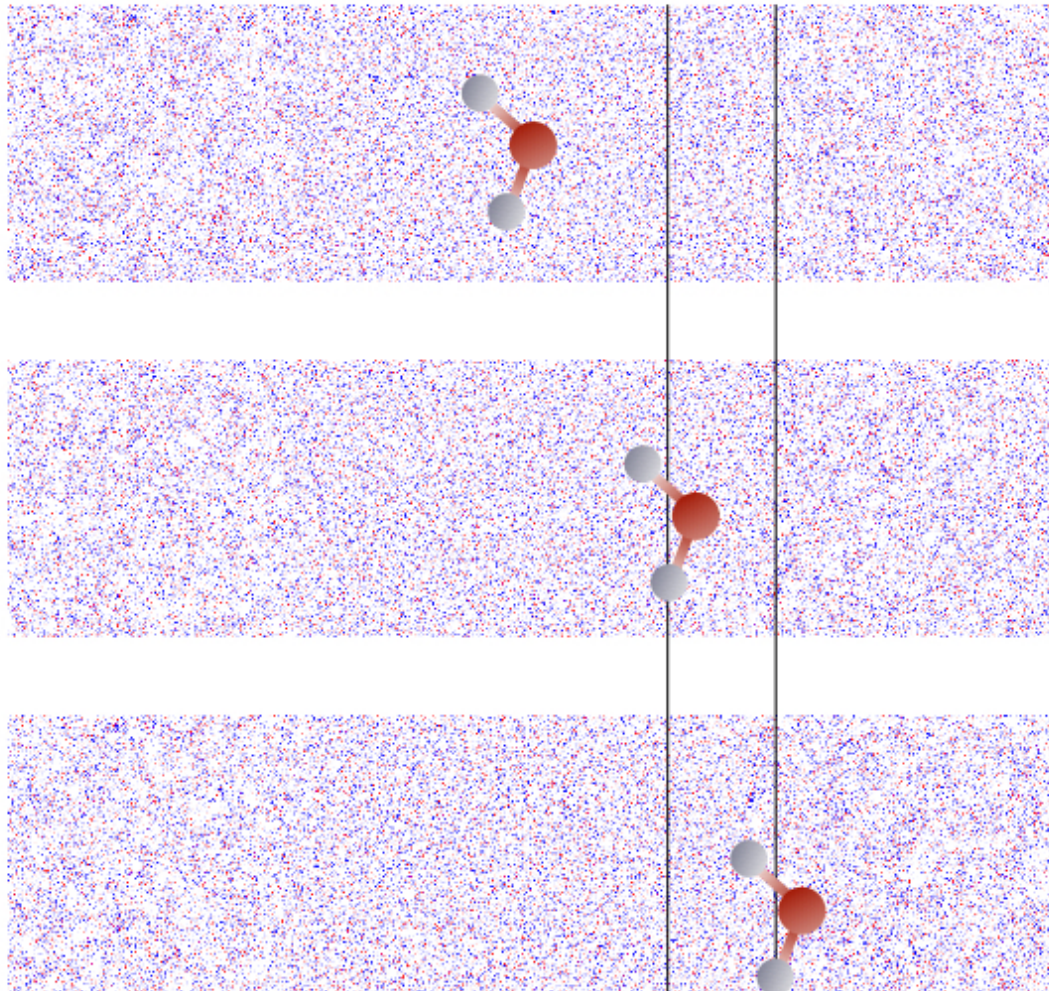
The FEC is the chemical potential difference between high and low resolution model

**If the CG model is an ideal gas,
the FEC equates the excess chemical potential**



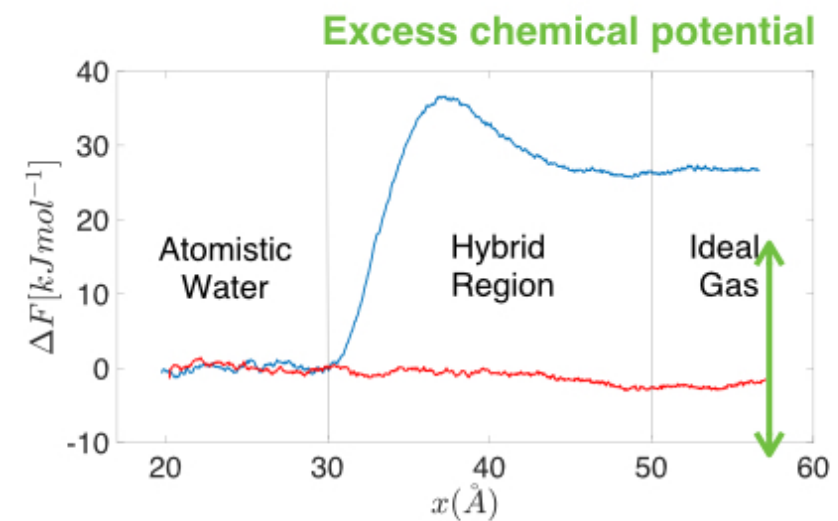
M. Heidari, K. Kremer, R. Cortes-Huerto and RP, submitted

Fast calculation of solvation free energy

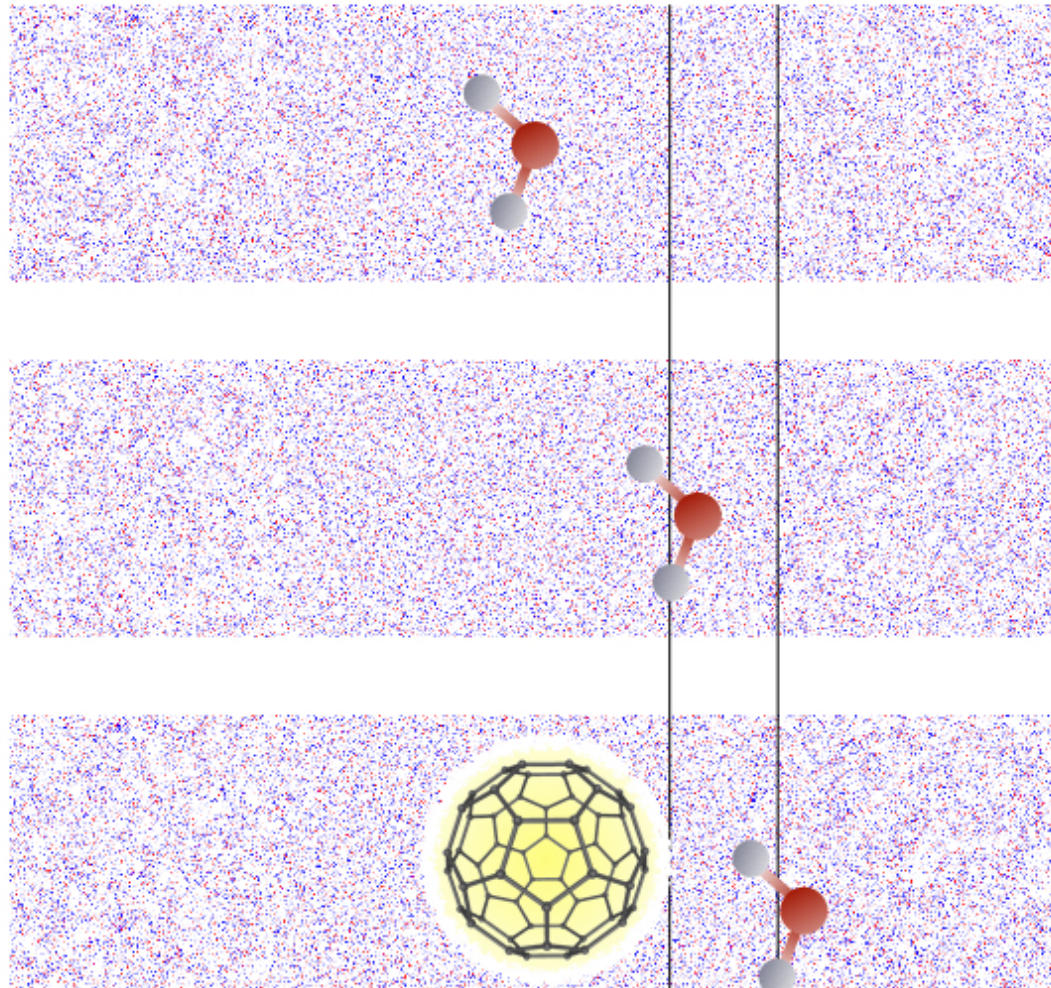


Pulling a molecule from the all-atom to the ideal gas region allows us to compute the excess chemical potential.

This approach is simple and effective especially for large molecules, such as fullerenes (ongoing work).

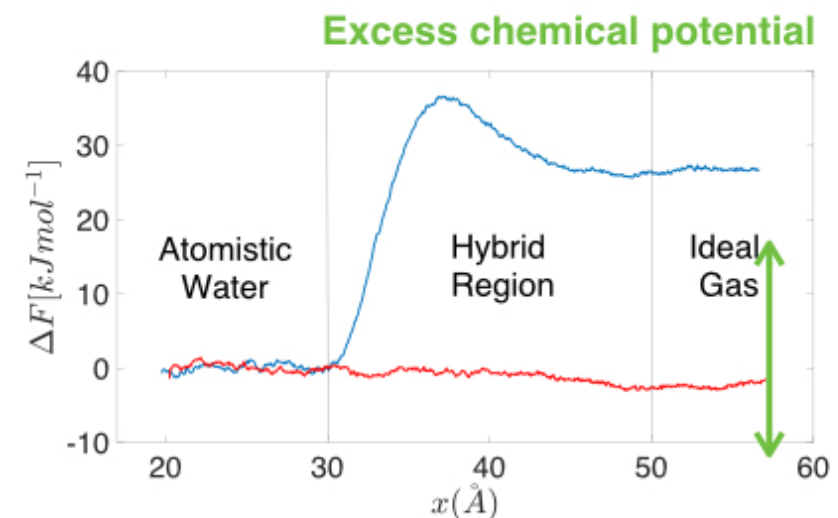


Fast calculation of solvation free energy

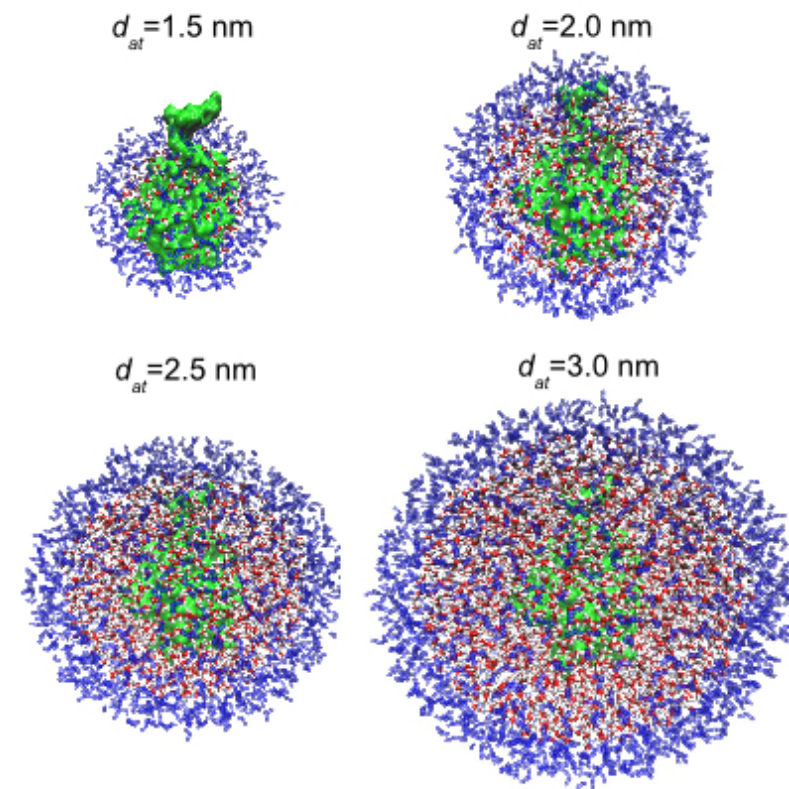
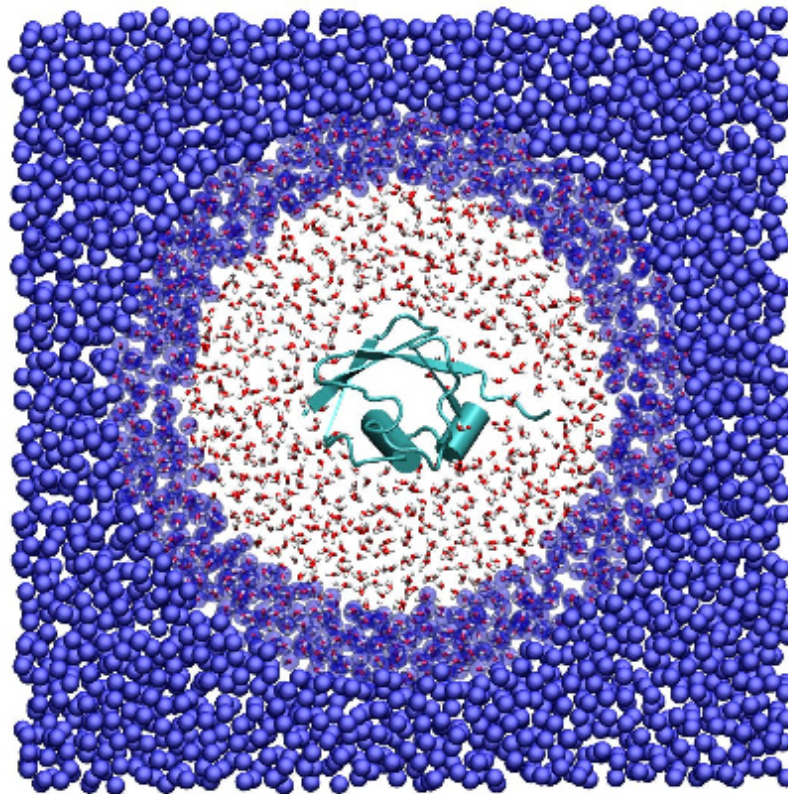


Pulling a molecule from the all-atom to the ideal gas region allows us to compute the excess chemical potential.

This approach is simple and effective especially for large molecules, such as fullerenes (ongoing work).

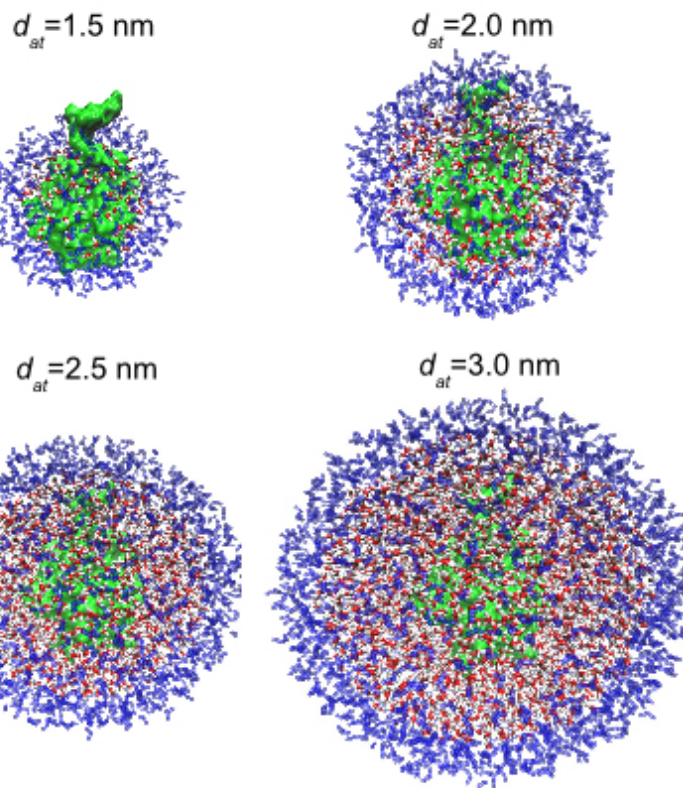
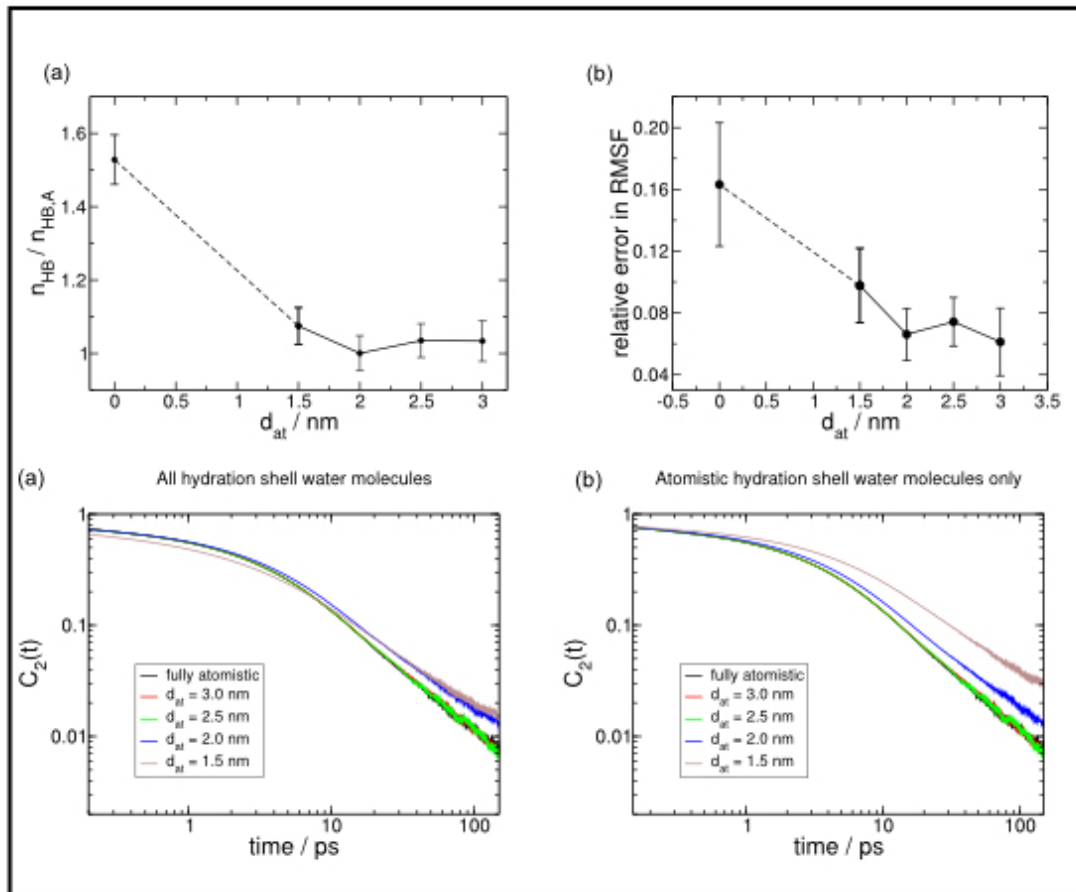


Ubiquitin in dual-res water

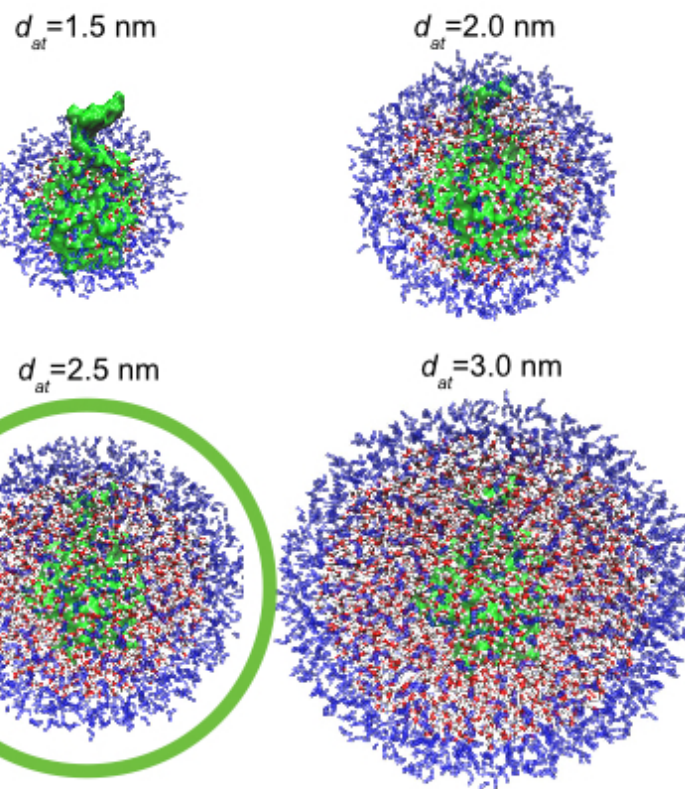
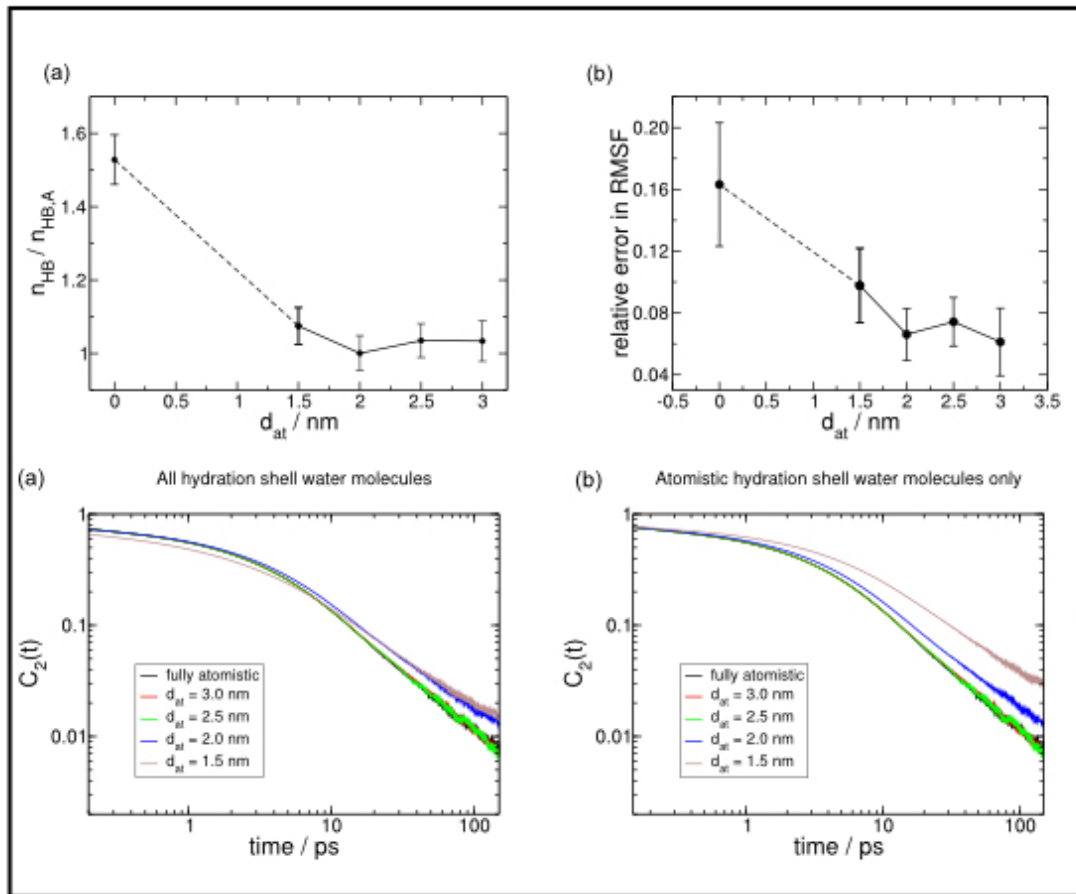


A.C. Fogarty, R.P., K. Kremer, JCP (2015)

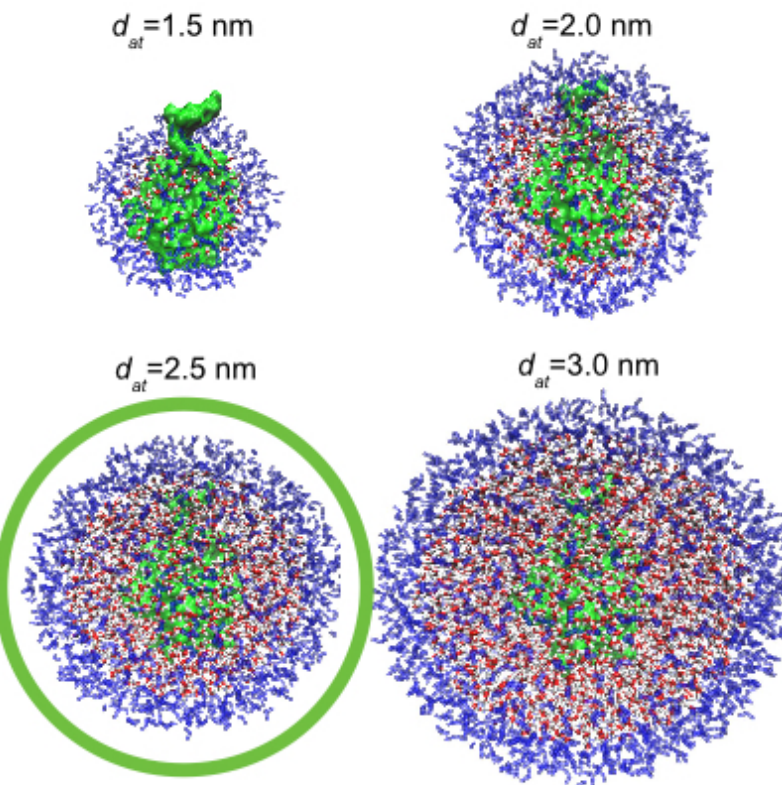
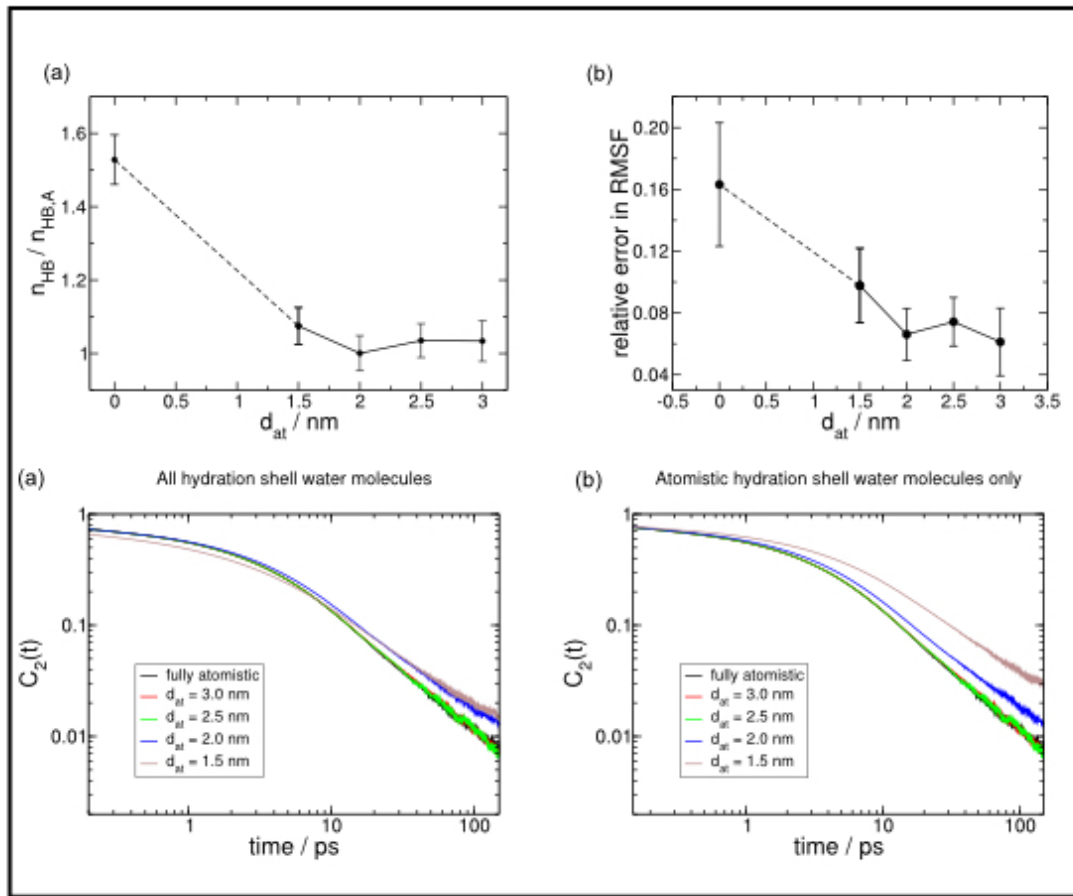
Ubiquitin in dual-res water



Ubiquitin in dual-res water

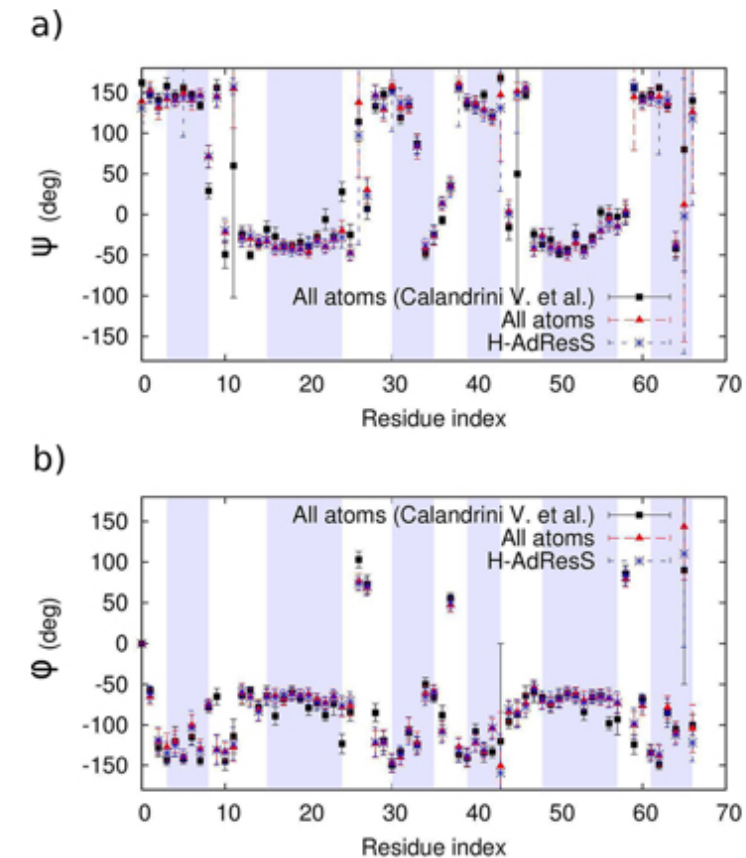
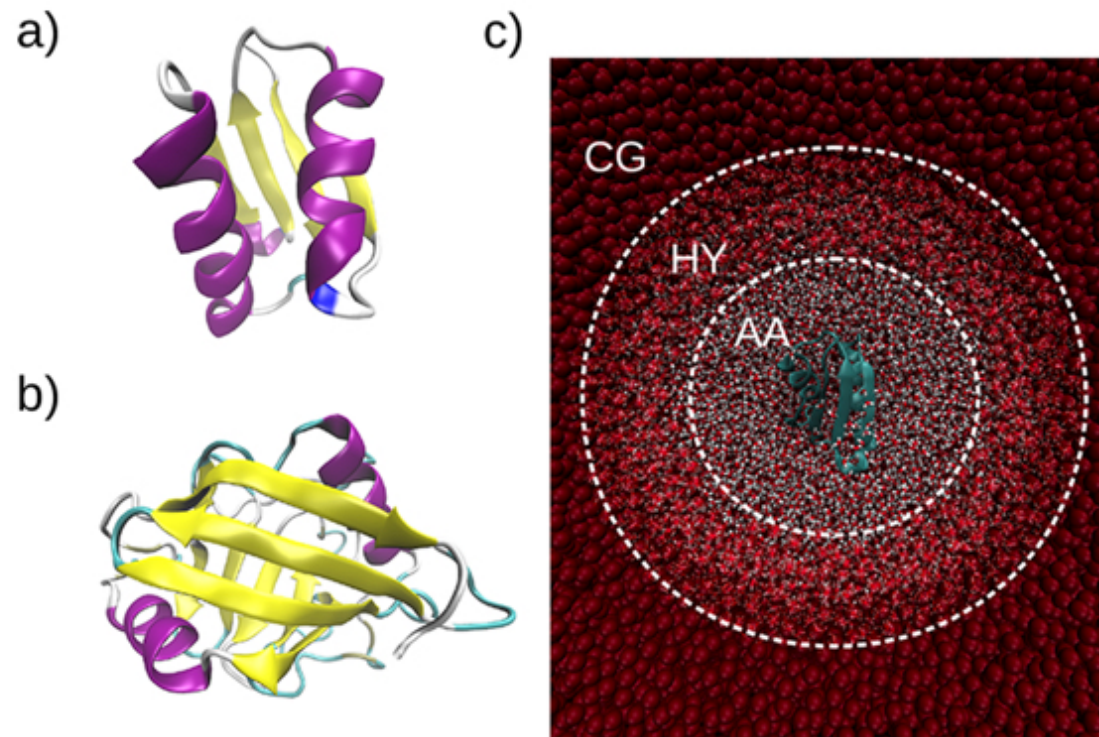


Ubiquitin in dual-res water



A ~1.3 nm thick water layer is sufficient
to reproduce the reference values of the observables under exam

Hamiltonian simulations of human metallochaperone atox1 and the human cyclophilin J in dual-res water

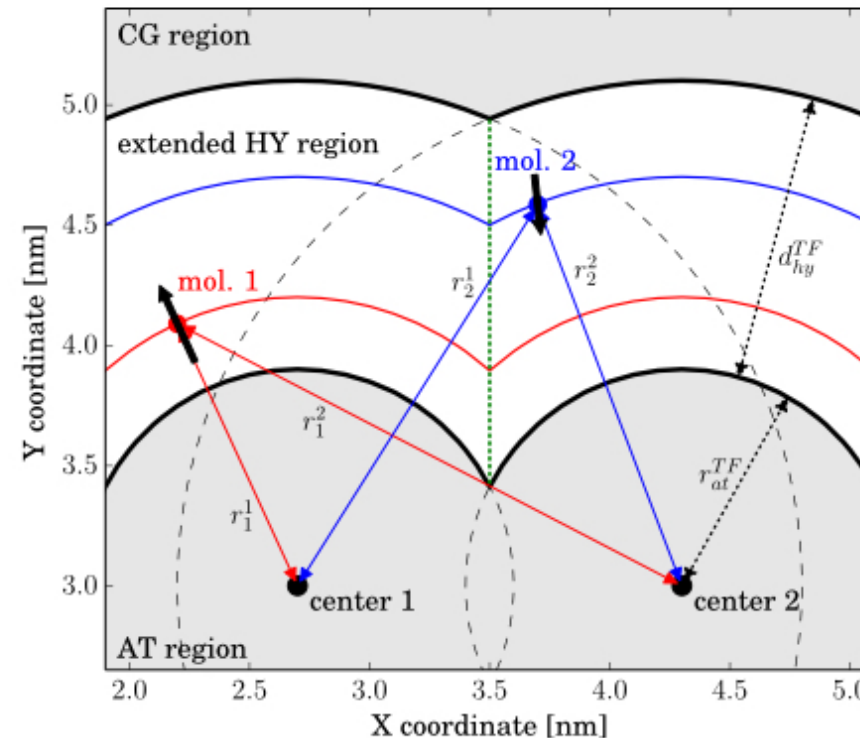
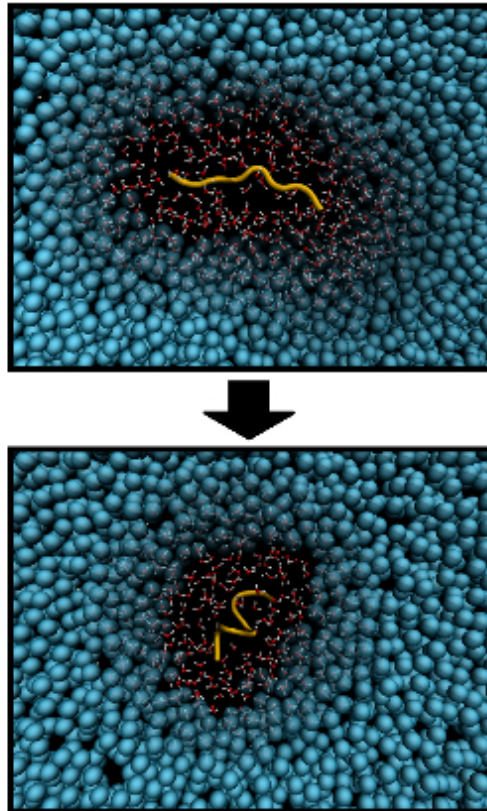


T. Tarenzi, V. Calandrini, R.P., A. Giorgetti, P. Carloni, JCTC (2017)

Adaptive adaptiveness

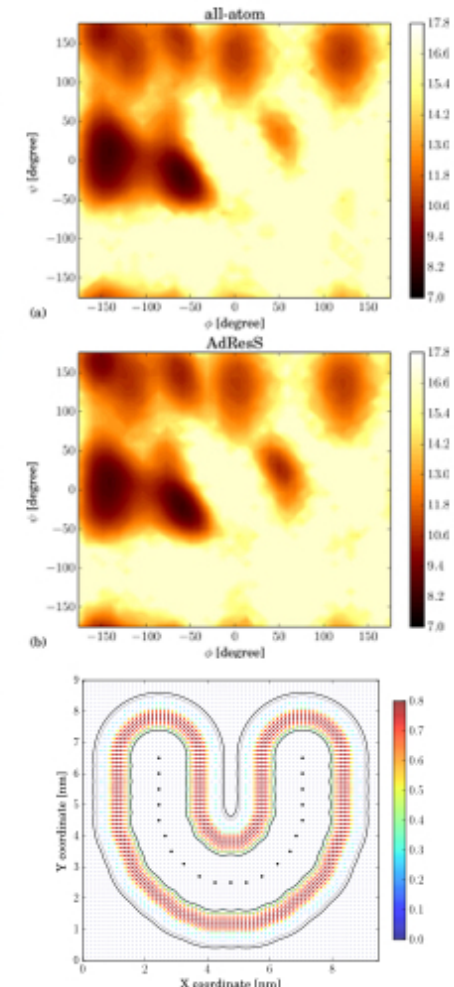
self-adjusting atomistic region in dual-resolution simulations

Peptide folding:
the smallest necessary
AT region size is not constant



The full AT region is the union of several spherical AT subdomains

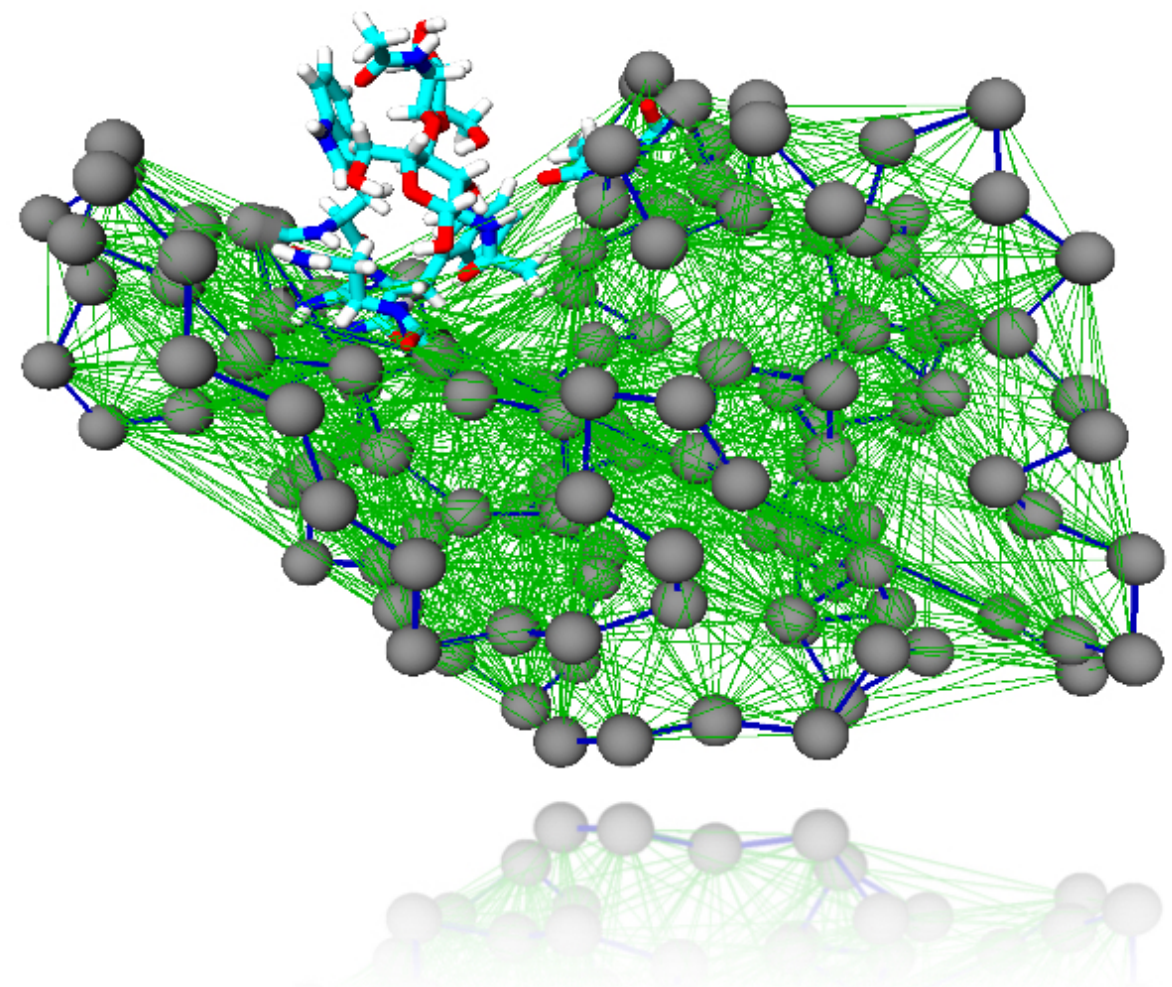
Structural and dynamical properties are preserved



Dual-resolution model of lysozyme

Atomistic resolution:
active site, ligand,
neighbouring solvent

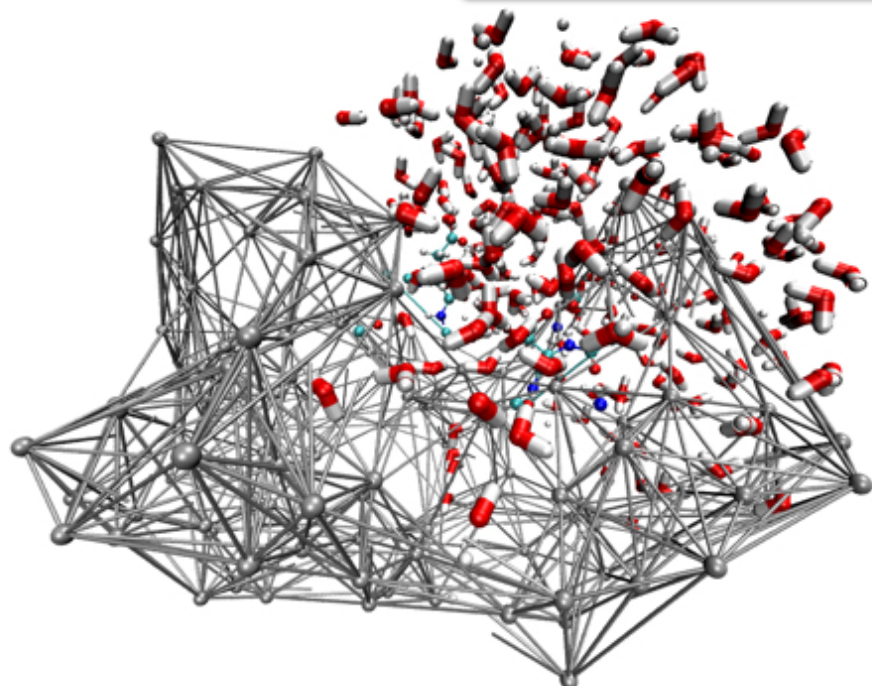
CG resolution:
protein *scaffold* and
rest of the solvent



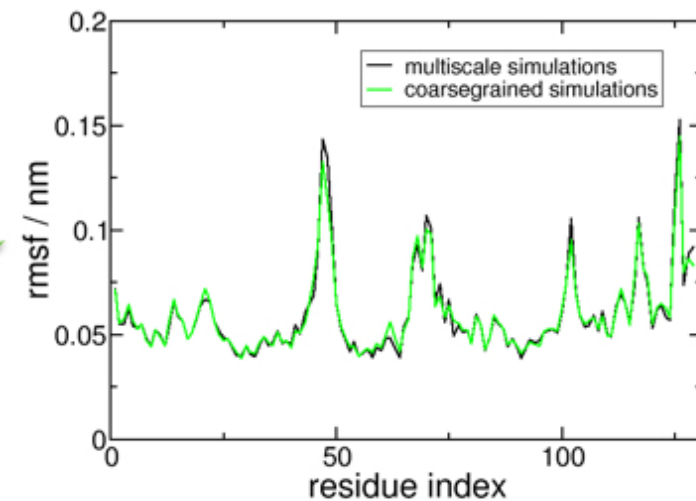
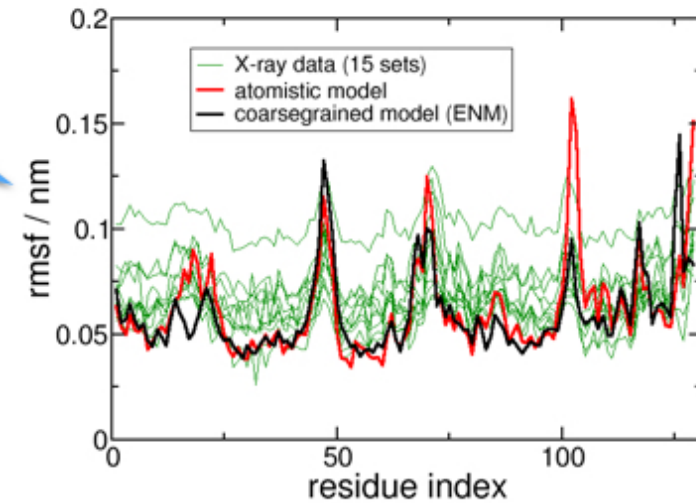
A.C. Fogarty, R.P., K. Kremer, Proteins (2016)

Dual-resolution model of lysozyme

ENM parametrised to reproduce experimental and all-atom MD data

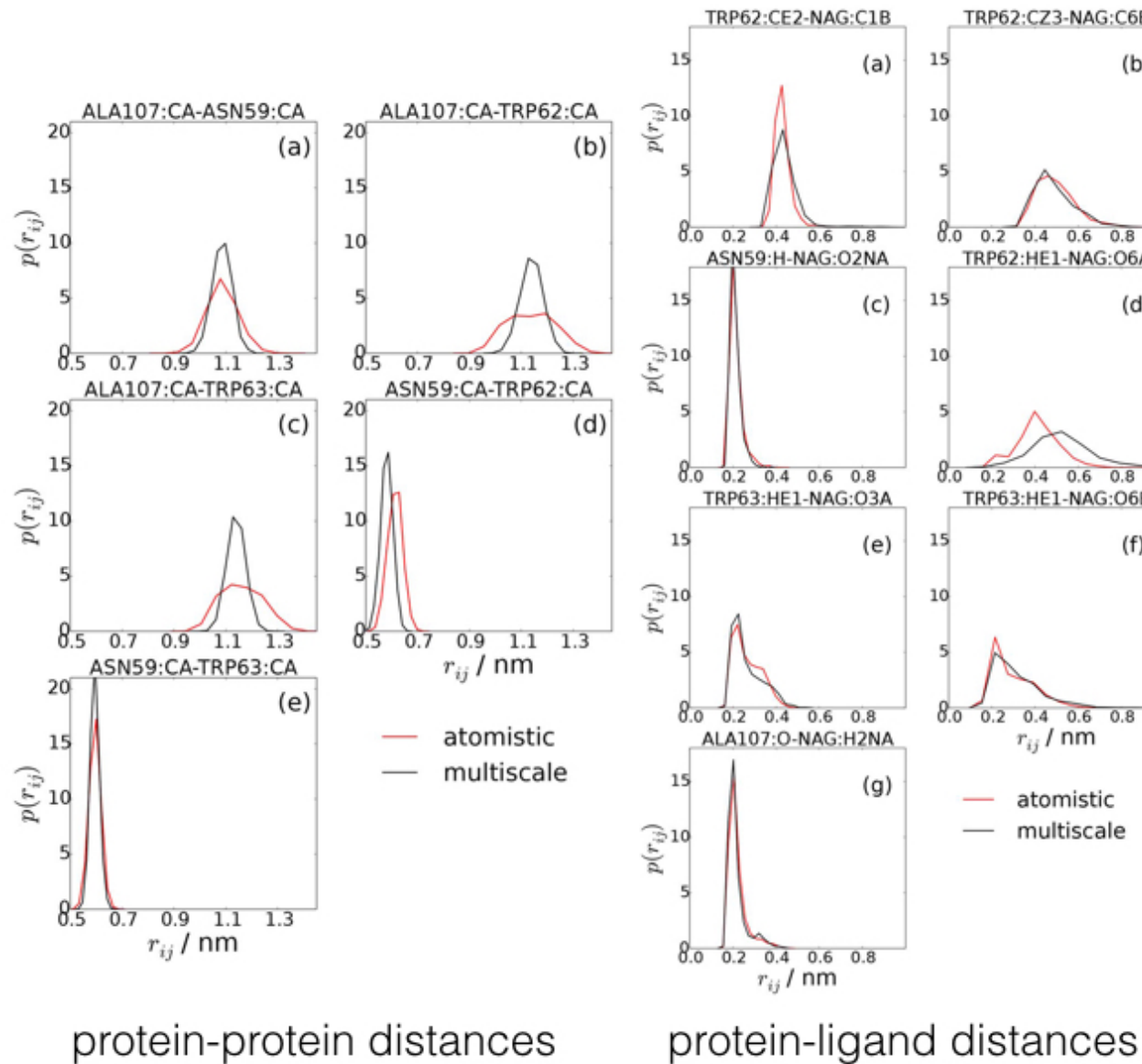


The dual-res system reproduces the global fluctuations of the ENM

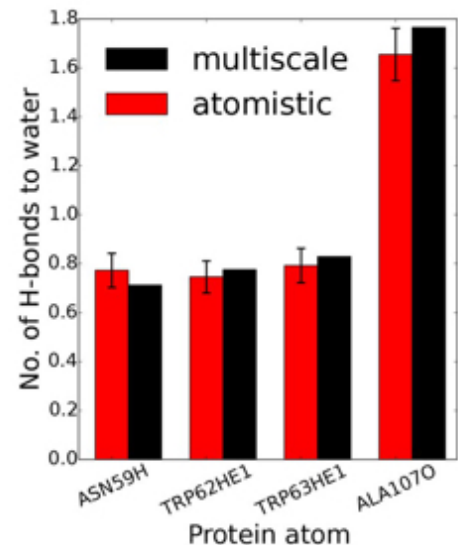
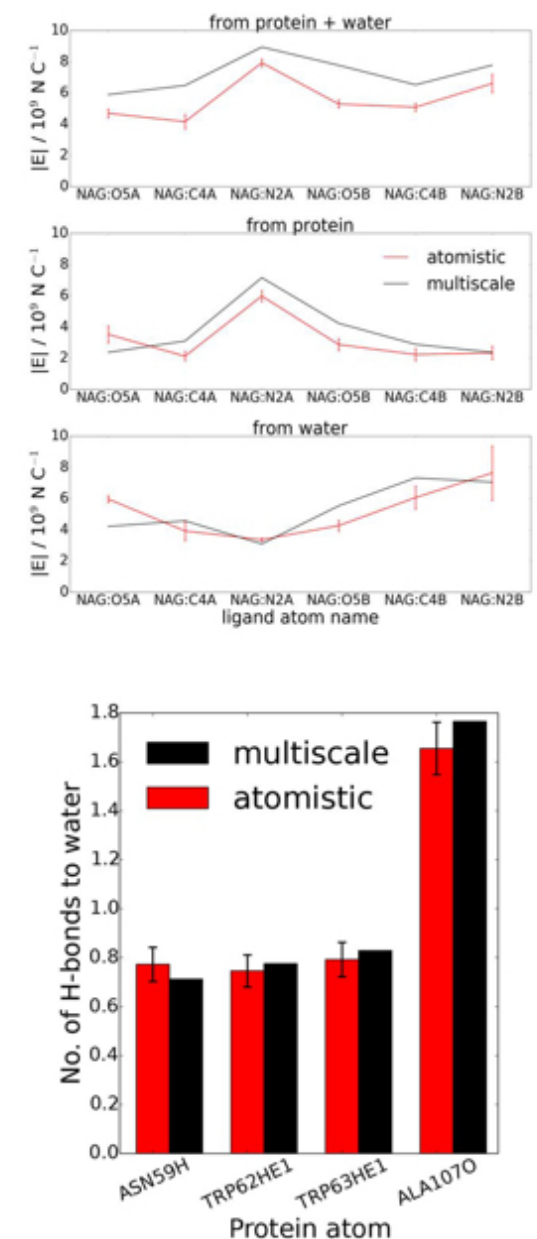


A.C. Fogarty, R.P., K. Kremer, Proteins (2016)

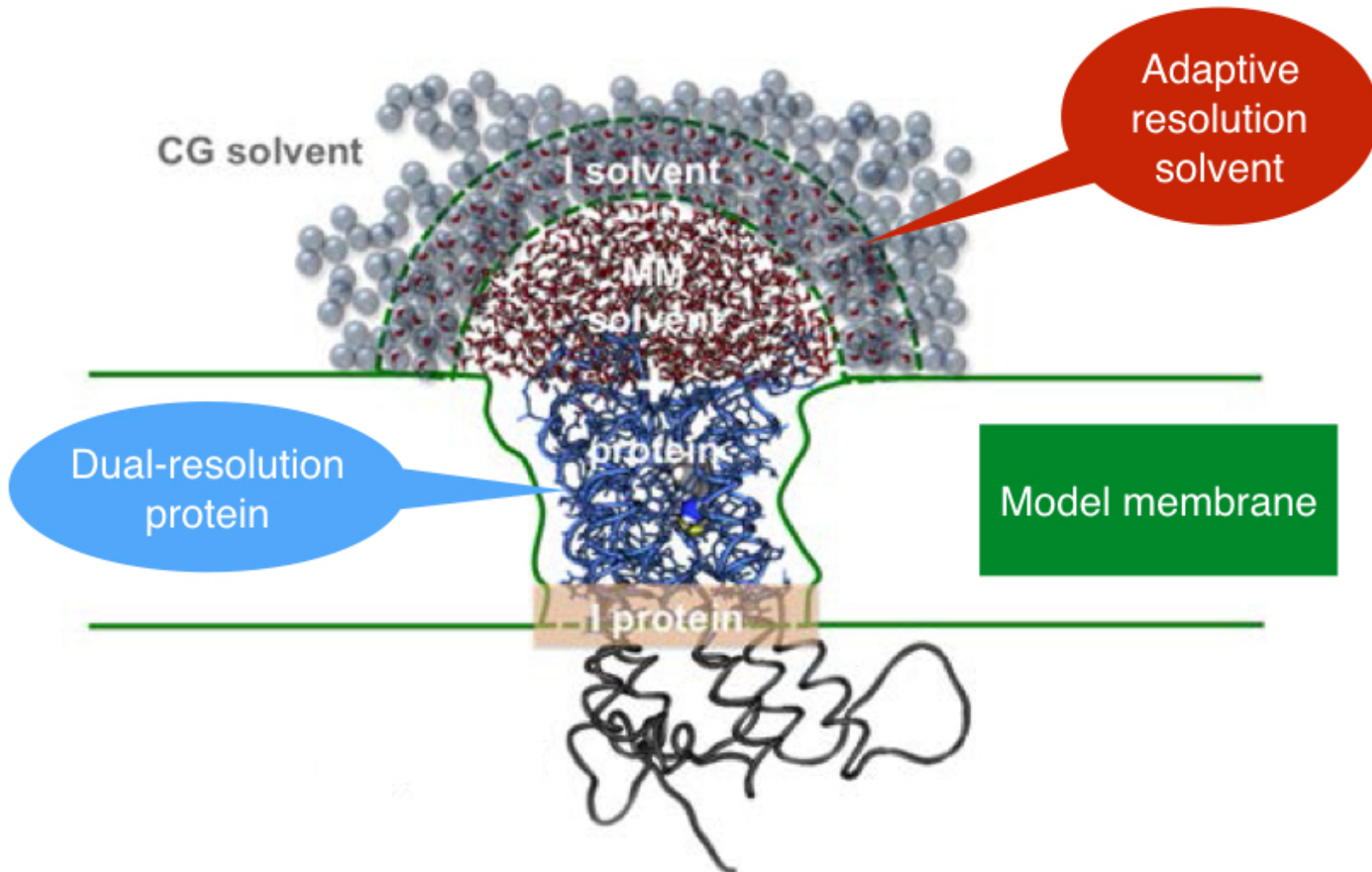
Dual-resolution model of lysozyme



A.C. Fogarty, R.P., K. Kremer, Proteins (2016)



Perspective: large size applications

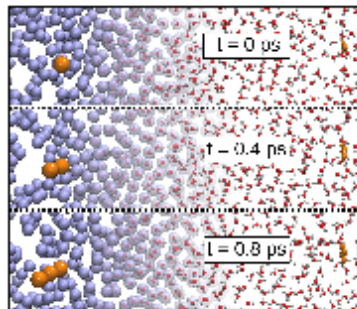


T. Tarenzi, V. Calandrini, R.P., A. Giorgetti, P. Carloni, JCTC 2017

Areas of application of adaptive resolution simulations methods

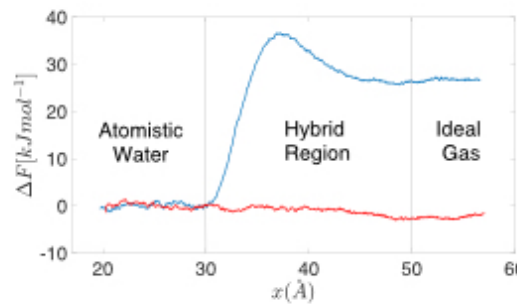
Fundamental Statistical Physics

Adaptive resolution simulation methods to study the stat mech of CG models



K. Kreis, A.C. Fogarty, K. Kremer, RP, EPJ-ST 2015

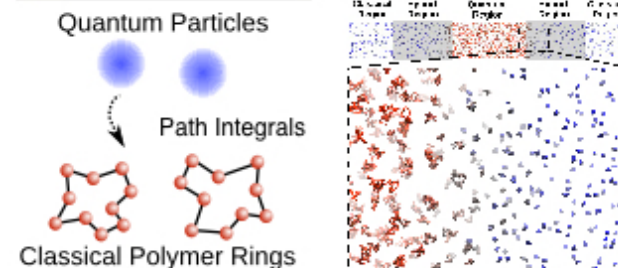
Efficient free energy calculations via adaptive resolution methods



M. Heidari, K. Kremer, R. Cortes Huerto, RP, submitted

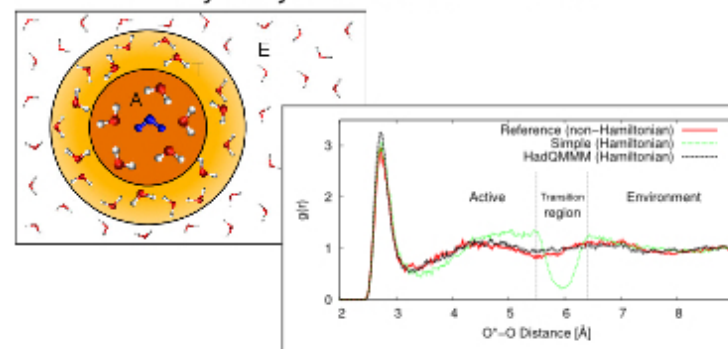
Quantum/Classical coupling

Hybrid quantum/classical models based on adaptive resolution simulation methods



K. Kreis, M. E. Tuckerman, D. Donadio, K. Kremer and RP, JCTC 2016

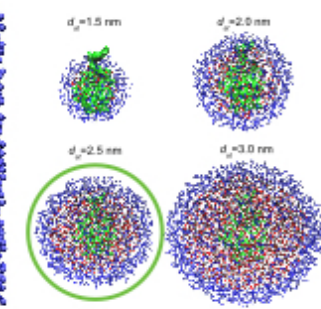
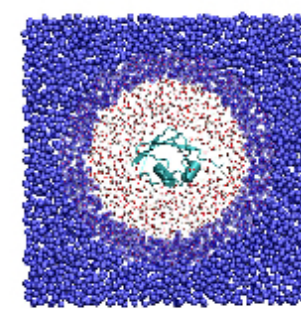
Hamiltonian QM/MM methods based on a many-body extension of H-AdResS



J. Boereboom, RP, D. Donadio, R. Bulo, JCTC 2016

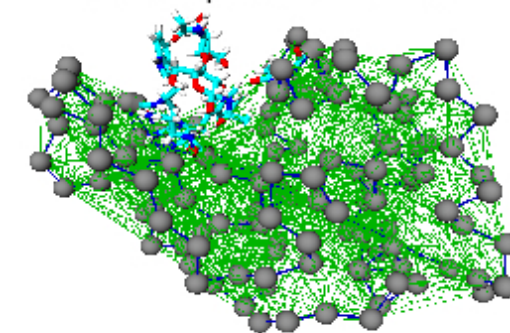
Biomolecule modeling and simulation

Dual-resolution simulation methods for biomolecular systems



A.C. Fogarty, R.P., K. Kremer, JCP 2015

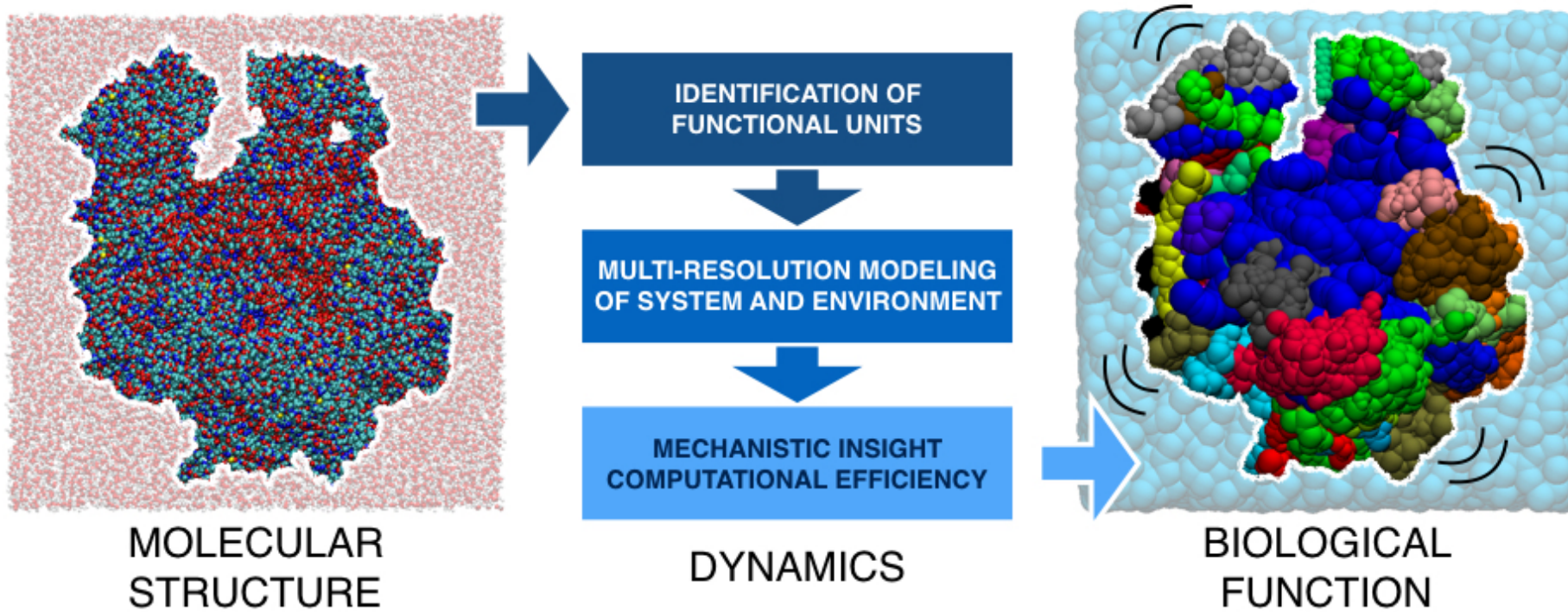
Dual-resolution models of a protein and its aqueous environment



A.C. Fogarty, RP and K. Kremer, Proteins 2016

The big picture

Road map towards the systematic
multi-resolution modelling of large biomolecules



Conclusions and perspectives

Conclusions and perspectives

- The complex behaviour of biological systems emerges from the **interplay of processes** occurring at different length and time scales

Conclusions and perspectives

- The complex behaviour of biological systems emerges from the **interplay of processes** occurring at different length and time scales
- **Systematic coarse-graining** methods provide valuable insight on the system properties

Conclusions and perspectives

- The complex behaviour of biological systems emerges from the **interplay of processes** occurring at different length and time scales
- **Systematic coarse-graining** methods provide valuable insight on the system properties
- **Large (supra)molecules pose new challenges** (large size, complex function)

Conclusions and perspectives

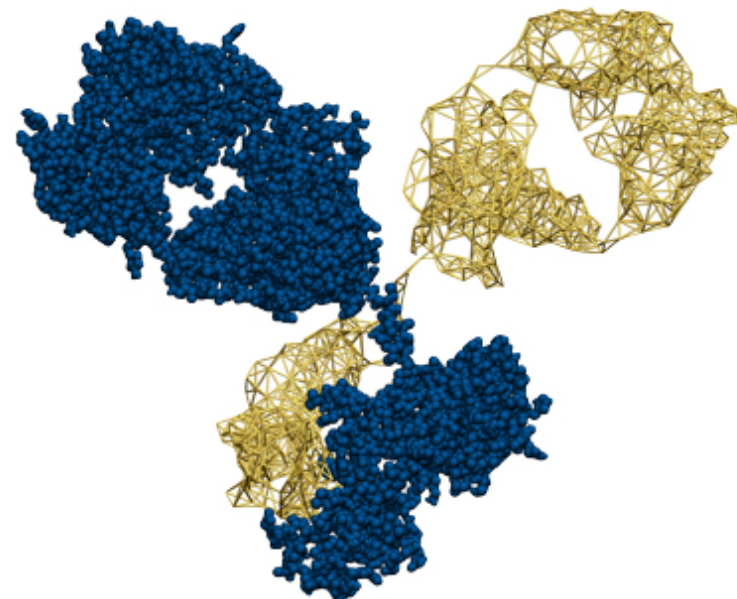
- The complex behaviour of biological systems emerges from the **interplay of processes** occurring at different length and time scales
- **Systematic coarse-graining** methods provide valuable insight on the system properties
- **Large (supra)molecules pose new challenges** (large size, complex function)
- **“One-size-blurs-all” CG models are too crude** (different system parts require a tailored description)

Conclusions and perspectives

- The complex behaviour of biological systems emerges from the **interplay of processes** occurring at different length and time scales
- **Systematic coarse-graining** methods provide valuable insight on the system properties
- **Large (supra)molecules pose new challenges** (large size, complex function)
- **“One-size-blurs-all” CG models are too crude** (different system parts require a tailored description)
- **Combination of various modelling strategies** for a local system-based modelling

ERC project VARIAMOLS

Variable resolution algorithms for macromolecular simulations



- Start date: January 1st, 2018
- Project goal: develop and apply novel techniques to represent a large biomolecule with models that are at the same time chemically accurate and computationally efficient
- **Open positions available! 2 Phd students + 2 postdocs in 2018 only**
- For info and openings visit: sites.google.com/view/variamols
- Email: variamols@unitn.it
- Facebook: facebook.com/variamols
- Twitter: [@r_potestio](https://twitter.com/r_potestio)

